

1 Vocal complexity in the long calls of Bornean orangutans

2

3 \*Erb, W.M.<sup>1,2</sup>, Ross, W.<sup>1</sup>, Kazanecki, H.<sup>1</sup>, Mitra Setia, T.<sup>3,4</sup>, Madhusudhana, S.<sup>1,5</sup>, Clink, D.J.<sup>1</sup>

4 \*Corresponding author

5 Email: [erbivorous@gmail.com](mailto:erbivorous@gmail.com)

6

7 <sup>1</sup> K. Lisa Yang Center for Conservation Bioacoustics, Cornell Lab of Ornithology, Cornell

8 University, Ithaca, New York, 14850, USA

9 <sup>2</sup> Department of Anthropology, Rutgers University, New Brunswick, New Jersey, 08901, USA

10 <sup>3</sup> Fakultas Biologi, Universitas Nasional Jakarta, Jakarta, Indonesia

11 <sup>4</sup> Primate Research Center, Universitas Nasional, Jakarta, Indonesia

12 <sup>5</sup> Centre for Marine Science and Technology, Curtin University, Perth, WA 6102, Australia

13

14 Short title: Orangutan Long Call Classification

15

## 16 **ABSTRACT**

17 Vocal complexity is central to many evolutionary hypotheses about animal communication. Yet,

18 quantifying and comparing complexity remains a challenge, particularly when vocal types are highly

19 graded. Male Bornean orangutans (*Pongo pygmaeus wurmbii*) produce complex and variable “long call”

20 vocalizations comprising multiple sound types that vary within and among individuals. Previous

21 studies described six distinct call (or pulse) types within these complex vocalizations, but none

22 quantified their discreteness or the ability of human observers to reliably classify them. We studied

23 the long calls of 13 individuals to: 1) evaluate and quantify the reliability of audio-visual classification

24 by three well-trained observers, 2) distinguish among call types using supervised classification and

25 unsupervised clustering, and 3) compare the performance of different feature sets. Using 46 acoustic  
26 features, we used machine learning (i.e., support vector machines, affinity propagation, and fuzzy c-  
27 means) to identify call types and assess their discreteness. We also used Uniform Manifold  
28 Approximation and Projection (UMAP) to visualize the separation of pulses using both extracted  
29 features and spectrograms. We found low inter-observer reliability and poor classification accuracy  
30 using supervised approaches, indicating that pulse types were not discrete. We propose a new pulse  
31 type classification scheme that is highly reproducible across observers and exhibits high classification  
32 accuracy using support vector machines. Although the low number of call types suggests long calls  
33 are fairly simple, the continuous gradation of sounds seems to greatly boost the complexity of this  
34 system. This work responds to calls for more quantitative research to define call types and measure  
35 the gradedness of animal vocal systems and highlights the need for a more comprehensive  
36 framework for studying vocal complexity vis-à-vis graded repertoires.

37

## 38 **HIGHLIGHTS**

- 39 ● We used audio-visual (AV) analysis and machine-learning to discriminate pulse types.
- 40 ● AV and support vector machines (SVM) did not support the six published pulse types.
- 41 ● Hard and soft clustering algorithms showed a mixture of discrete and graded pulses.
- 42 ● We propose three pulse types that show high reproducibility and classification accuracy.
- 43 ● More work is needed to investigate the role of graded signals in vocal complexity.

44

## 45 **KEYWORDS**

46 acoustic communication; affinity propagation; fuzzy clustering; graded signals; machine learning;  
47 supervised classification; support vector machines; Uniform Manifold Approximation and  
48 Projection (UMAP); unsupervised clustering; vocal repertoire

## 49 INTRODUCTION

50           Vocal complexity, or the diversity of sounds in a species' repertoire, is central to many  
51 evolutionary hypotheses about animal communication (Bradbury & Vehrencamp, 2011; Fischer et  
52 al., 2016; Freeberg et al., 2012; McComb & Semple, 2005). This complexity has been hypothesized  
53 to be shaped by a range of factors including predation pressure, sexual selection, habitat structure,  
54 and social complexity (Bradbury & Vehrencamp, 2011; Fischer et al., 2016). Two common measures  
55 of vocal complexity are: 1) the diversity (or number) of call types as well as 2) their discreteness. For  
56 instance, within black-capped chickadee (*Poecile atricapillus*) groups, individuals flexibly increase the  
57 diversity of note types when they are in larger groups, presumably increasing the number of  
58 potential messages that can be conveyed (Freeberg et al., 2012). When comparing across species,  
59 similar themes emerge in rodents and primates. Sciurid species with a greater diversity of social roles  
60 have more alarm call types (Blumstein & Armitage, 1997) and primate species in larger groups with  
61 more intense social bonding have larger vocal repertoires (McComb & Semple, 2005). Further, it has  
62 been proposed that while discrete repertoires facilitate signal recognition in dense habitats, graded  
63 calls allow more complexity in open habitats where intermediate sounds communicate arousal and  
64 can be linked with visual signals (Marler et al., 1975).

65           Yet, quantifying vocal complexity in a standardized manner remains a challenge for  
66 comparative analyses. A primary aspect of this challenge is related to the identification and  
67 quantification of discrete call types, which is particularly vexing in repertoires comprising  
68 intermediate calls and in species that exhibit significant inter-individual variation (Fischer et al.,  
69 2016). The most common approaches to identifying call types are: 1) manual (visual or audio-visual)  
70 classification of spectrograms by a human observer and 2) automated (quantitative or algorithmic)  
71 using features that are either manually or automatically measured from spectrograms (Kershenbaum  
72 et al., 2016). Audio-visual classification involves one or more observers inspecting spectrograms

73 visually while simultaneously listening to the sounds. This method has been applied to the  
74 vocalizations of numerous taxa (e.g., manatees, *Trichechus manatus latirostris*: Brady et al., 2020; spear-  
75 nosed bats, *Phyllostomus discolor*: Lattenkamp, 2019; humpback whales, *Megaptera novaeangliae*:  
76 Madhusudhana et al., 2019; New Zealand kea parrots, *Nestor notabilis*: Schwing et al., 2012). Audio-  
77 visual classification studies often rely on a single expert observer and only rarely quantify within- or  
78 between-observer reliability (reviewed in Jones et al., 2001). On one hand, when classification is  
79 done by a single observer, the study risks idiosyncratic or irreproducible results. On the other hand,  
80 when multiple observers are involved, the study risks inconsistent assessments among scorers. To  
81 assess the reproducibility of a human-based classification scheme, it is critical to evaluate the  
82 consistency of scores within and/or among the human observers using inter-rater reliability (IRR)  
83 statistics such as Cohen's kappa (Hallgren, 2012).

84 To compare and classify acoustic signals, researchers must make decisions about which  
85 features to estimate, as analyses of the waveform are generally too computationally costly. A  
86 commonly used approach for many classification problems is feature selection, in which a suite of  
87 selected time- and frequency-based characteristics of sounds are measured and compiled from  
88 manually annotated spectrograms (Odom et al., 2021). There is little standardization concerning the  
89 selection of acoustic variables across studies, which often include a combination of qualitative and  
90 quantitative measurements that are manually and/or automatically (i.e., using a sound analysis  
91 program, such as Raven Pro 1.6) extracted. As an alternative to feature selection, some researchers  
92 use automated approaches wherein the spectral content of sounds is measured using spectrograms,  
93 cepstra, multi-taper spectra, wavelets, or formants (reviewed in Kershenbaum et al., 2016).

94 Once features have been manually or automatically extracted, multivariate analyses can be  
95 used to classify or cluster sounds using supervised or unsupervised algorithms, respectively. In the  
96 case of supervised classification, users manually label a subset of representative sounds which are

97 used to train the statistical model that will subsequently be used to automatically identify those  
98 sound types in an unlabeled set of data (Cunningham et al., 2008). In contrast to supervised  
99 classification, clustering is an unsupervised machine learning approach in which an algorithm divides  
100 a dataset into several groups or clusters such that observations in the same group are similar to each  
101 other and dissimilar to the observations in different groups (Greene et al., 2008). Thus, in the case of  
102 unsupervised clustering, the computer – rather than the human observer – learns the groupings and  
103 assigns labels to each value (Alloghani et al., 2020).

104 Enumeration of call types in a repertoire is especially challenging when there are  
105 intermediate forms that fall between categories. These so-called graded call types have been well  
106 documented across primate taxa (Fischer et al., 2016; Hammerschmidt & Fischer, 1998). An  
107 alternative to “hard clustering” of calls into discrete categories (e.g., k-means, k-medoids, affinity  
108 propagation), “soft clustering” (e.g., fuzzy c-means) allows for imperfect membership by assigning  
109 probability scores for membership in each cluster, thereby making it possible to identify call types  
110 with intermediate values (Cusano et al., 2021; Fischer et al., 2016). So-called fuzzy clustering can be  
111 used in tandem with hard clustering by also quantifying the degree of ambiguity (or gradedness)  
112 exhibited by particular sounds and continuities across call types. Thus, soft clustering provides a  
113 means of quantifying gradedness in repertoires and can enable the identification of intermediate  
114 members.

115 Across studies of animal vocal complexity, there is notable variation in the number and type  
116 of feature sets used, ranging from fewer than 10 to more than 100 parameters that are manually  
117 and/or automatically extracted. Table 1 provides a summary of 15 studies across mammalian and  
118 avian taxa that used supervised classification and unsupervised clustering approaches to identify call  
119 types across a range of mammalian and avian taxa. Though most studies paired audio-visual  
120 classification with an unsupervised clustering method, a few also included discriminant function

121 analysis (DFA) to quantify the differences among the human-labeled call types and/or computer-  
122 identified clusters. Authors relied on a broad range of unsupervised clustering algorithms, though  
123 hierarchical agglomerative clustering was the most used method. Studies that aimed to provide an  
124 accurate classification of different call types often relied on a combination of supervised  
125 classification and unsupervised clustering methods to ensure results were robust and repeatable.  
126 However, those that compared feature sets or clustering methods often reported a lack of agreement  
127 on the number of clusters identified, highlighting the difficulty of the seemingly straightforward task  
128 of identifying and quantifying call types.

129 **Table 1.** Review of studies using supervised classification and unsupervised clustering approaches to identify vocal types.

Authors (Date)	Taxon	Goals	N Features	Classification (N observers)	Clustering Method
Wadewitz et al. (2015)	Chacma baboon ( <i>Papio ursinus</i> )	Compare hard & soft clustering, evaluate influence of features	9, 38, 118 (+ 19 PCA factors)	A/V *	K-means, Hierarchical agglomerative (Ward's), Fuzzy c-means
Fuller (2014)	Blue monkey ( <i>Cercopithecus mitis stuhlmanni</i> )	Catalog vocal signals	18 PCA factors	A/V (1), DFA **	Hierarchical agglomerative
Fournet et al., (2015)	Humpback whale ( <i>Megaptera novaeangliae</i> )	Catalog non-song vocalizations	15	A/V (1), DFA	Hierarchical agglomerative
Brady et al. (2020)	Florida manatee ( <i>Trichechus manatus latirostris</i> )	Catalog vocal repertoire	17	A/V (1)	Maximum likelihood, CART
Hammerschmidt & Fischer (2019)	Chacma ( <i>Papio ursinus</i> ), olive ( <i>P. anubis</i> ), and Guinea baboon ( <i>P. papio</i> )	Catalog & compare vocal repertoires, Compare A/V to clustering	9	A/V (multiple), DFA **	Two-step cluster analysis
Sadhukhan et al. (2019)	Indian wolf ( <i>Canis lupus pallipes</i> )	Catalog harmonic vocalizations	8	DFA	Hierarchical agglomerative
Hedwig et al. (2019)	African forest elephant ( <i>Loxodonta cyclotis</i> )	Catalog vocal repertoire	23	DFA **	PCA
Huijser et al. (2020)	Sperm whale ( <i>Physeter macrocephalus</i> )	Catalog coda repertoires	2	A/V (1)	K-means, Hierarchical agglomerative
Vester et al. (2017)	Long-finned pilot whale ( <i>Globicephala melas</i> )	Catalog vocal repertoire	14	A/V (2), DFA	Two-step cluster analysis

Soltis et al. (2012)	Key Largo woodrat ( <i>Neotoma floridana smalli</i> )	Catalog vocal repertoire	6	A/V*	Multidimensional scaling analysis (MDS)
Elie & Theunissen (2016)	Zebra finch ( <i>Taeniopygia guttata</i> )	Catalog vocal repertoire, determine distinguishing features	22, 25 (MFCCs)	A/V (1), Fisher LDA, Random Forest	PCA, Gaussian mixture
Janik (1999)	Bottlenose dolphin ( <i>Tursiops truncatus</i> )	Compare A/V to clustering	20	A/V (5)	K-means, Hierarchical agglomerative
Cusano et al. (2021)	Humpback whale ( <i>Megaptera novaeangliae</i> )	Differentiate discrete vs. graded call types	25	A/V*	Fuzzy k-means
Garland et al. (2015)	Beluga whale ( <i>Delphinapterus leucas</i> )	Catalog vocal repertoire	12	A/V*	CART, Random Forest
Thiebault et al. (2019)	Cape gannet ( <i>Morus capensis</i> )	Catalog repertoire of foraging calls	12	A/V*	Random Forest

130 \* Study did not report # of observers

131 \*\* leave-one-out



132           In the present study, we examine vocal complexity in the long calls of Bornean orangutans  
133 (*Pongo pygmaeus wurmbii*) by evaluating how the choice of classification or clustering methods and  
134 feature inputs affect the number of call types we recognize. Orangutans are semi-solitary great apes  
135 who exhibit a promiscuous mating system in which solitary adult males range widely in search of  
136 fertile females (Spillmann et al., 2017). Flanged males (i.e., adult males who have fully developed  
137 cheek pads, throat sacs, and body size approximately twice that of adult females) emit loud  
138 vocalizations, or long calls, which travel up to a kilometer and serve to attract female mates and  
139 repel rival males (Mitra Setia & van Schaik, 2007) In this social setting, long calls thus hold an  
140 important function for coordination among widely dispersed individuals.

141           Long calls are complex and variable vocalizations comprising multiple call (or pulse) types  
142 that vary within and among individuals (Askew & Morrogh-Bernard, 2016; Spillmann et al., 2010).  
143 Long calls typically begin with a bubbly introduction of soft, short sounds that build into a climax of  
144 high-amplitude frequency-modulated pulses followed by a series of lower-amplitude and -frequency  
145 pulses that gradually transition to soft and short sounds, similar to the introduction (cf. MacKinnon,  
146 1977, Table S1). Although Davilla Ross and Geissmann (2007) first attempted to classify and name  
147 the different elements of these calls, they noted a “wide variety of call elements do not belong to any  
148 of these note types” (Davila Ross & Geissmann, 2007 p. 309).

149           Spillmann and colleagues (2010) presented the most detailed description of orangutan long  
150 calls in which they identified six different pulse types (Table 2), but thus far there has been no  
151 attempt to systematically classify pulses or quantify how discrete these sounds are. Further, no  
152 studies have described the process for or the number of observers classifying sound types nor the  
153 reliability of classifications within or among observers. Thus, it is presently unclear how well pulse  
154 types can be discriminated by human observers or quantitative classification tools, thereby limiting  
155 our ability to repeat, reproduce, and replicate these studies.

156 **Table 2.** Names and descriptions of sound labels used in previous studies, using Spillmann et al.  
157 (2010) labels as reference.

<b>Sound Type</b>	<b>MacKinnon 1974</b>	<b>Davila Ross &amp; Geissmann 2007</b>	<b>Spillmann et al. 2010</b>
Grumbles	bubbly introduction	bubbling	“preceding bubbling-like elements that are low in loudness”
Bubbles	n/a	bubbling	“low amplitude, looks like a cracked sigh”
Roar	“climax of full roars”	roar	“more rounded and lower in frequency”
Low Roar	n/a	n/a	“half the fundamental frequency at the highest point than roar”
Volcano Roar	n/a	n/a	“sharp tip and higher frequency than roar”
Huitus	n/a	huitus	“high amplitude with steeply ascending and descending part that are not connected”
Intermediary	n/a	intermediary	“low amplitude, frequency modulation starts with a rising part followed by a falling part that changes again into a rising and ends with a falling part”
Sigh	“tails off gradually into a series of sighs”	sigh	“low amplitude, starts with a short rising part and changes in a long falling part”

158

159 The present study aims to evaluate vocal complexity in orangutan long calls to compare  
160 different approaches to identifying the number of discrete calls and estimating the degree of  
161 gradedness in a model vocal system. Specifically, the objectives of our study are to: 1) evaluate and  
162 quantify the reliability of manual audio-visual (AV) classification by three well-trained observers, 2)  
163 classify and cluster call types using supervised classification (support vector machines) and  
164 unsupervised hard (affinity propagation) and soft (fuzzy c-means) clustering methods, and 3)

165 compare the results using different feature sets (i.e., feature engineering, complete spectrographic  
166 representations). Based on these findings, we will make explore and assess alternative classification  
167 systems for identifying discrete and graded call types in this system.

168

## 169 **METHODS**

### 170 **Ethical Note**

171 This research was approved by the Institutional Animal Care and Use Committee of Rutgers,  
172 the State University of New Jersey (protocol number 11-030 granted to Erin Vogel). Permission to  
173 conduct the research was granted to WME by the Ministry of Research and Technology of the  
174 Republic of Indonesia (RISTEK Permit #137/SIP/FRP/SM/V/2013-2015). The data included in  
175 the present study comprise recordings collected during passive observations of wild habituated  
176 orangutans at distances typically exceeding 10 m. The population has been studied since 2003 and  
177 individual orangutans were not disturbed by observers in the execution of this study.

178

### 179 **Study Site and Subjects**

180 We conducted our research at the Tuanan Orangutan Research Station in Central  
181 Kalimantan, Indonesia (2<sup>0</sup> 09' 06.1" S; 114<sup>0</sup> 26' 26.3" E). Tuanan comprises approximately 900  
182 hectares of secondary peat swamp forest that was selectively logged prior to the establishment of the  
183 study site in 2003 (see Erb et al., 2018 for details). For the present study, data were collected  
184 between June 2013 and May 2016 by WME and research assistants (see Acknowledgments) during  
185 focal observations of adult flanged males. Whenever flanged males were encountered, our field team  
186 followed them until they constructed a night nest and we returned to the nest before dawn the next  
187 morning to continue following the same individual. All subjects were individually recognized on the  
188 basis of unique facial features, scars, and broken or missing digits. Individuals were followed

189 continuously for five days, unless they were lost or left the study area. During 316 partial- and full-  
190 day focal observations, we recorded 1,013 long calls from 23 known individuals.

191

## 192 **Long Call Recording**

193 During observations, we used all-occurrences sampling (Altmann, 1974) of long calls noting:  
194 time, GPS location, stimulus (preceded within 15 minutes by another long call, tree fall, approaching  
195 animal, or other loud sounds), and any accompanying movements or displays. Recordings of long  
196 calls were made opportunistically, using a Marantz PMD-660 solid-state recorder (44,100 Hz  
197 sampling frequency, 16 bits: Kanagawa, Japan) and a Sennheiser directional microphone (K6 power  
198 module and ME66 recording head: Wedemark, Germany). Observers made voice notes at the end of  
199 each recording noting the date and time, orangutan's name, height(s), distance(s), and movement(s),  
200 as well as the gain and microphone directionality (i.e., directly or obliquely oriented).

201

## 202 **Long Call Analysis**

203 For the present study, we selected a subset of recordings from 13 males from whom we had  
204 collected at least 10 high-quality long call recordings. When more than 10 long call recordings were  
205 available for a given individual, we randomly selected 10 of his recordings, stratified by study year, to  
206 balance our dataset across individuals and years. The final dataset comprised 130 long calls, 10 from  
207 each of 13 males.

208 Prior to annotating calls, we used Adobe Audition 14.4 to downsample recordings to 5,100  
209 Hz (cf. Hammerschmidt & Fischer, 2019). We then generated spectrograms in Raven Pro 1.6 (K.  
210 Lisa Yang Center for Conservation Bioacoustics, 2019) with a 512-point (92.9 ms) Hann window (3  
211 dB bandwidth = 15.5 Hz), with 90% overlap and a 512-point DFT, yielding time and frequency  
212 measurement precision of 9.25 ms and 10.8 Hz. Three observers (WME, WR, HK) annotated calls

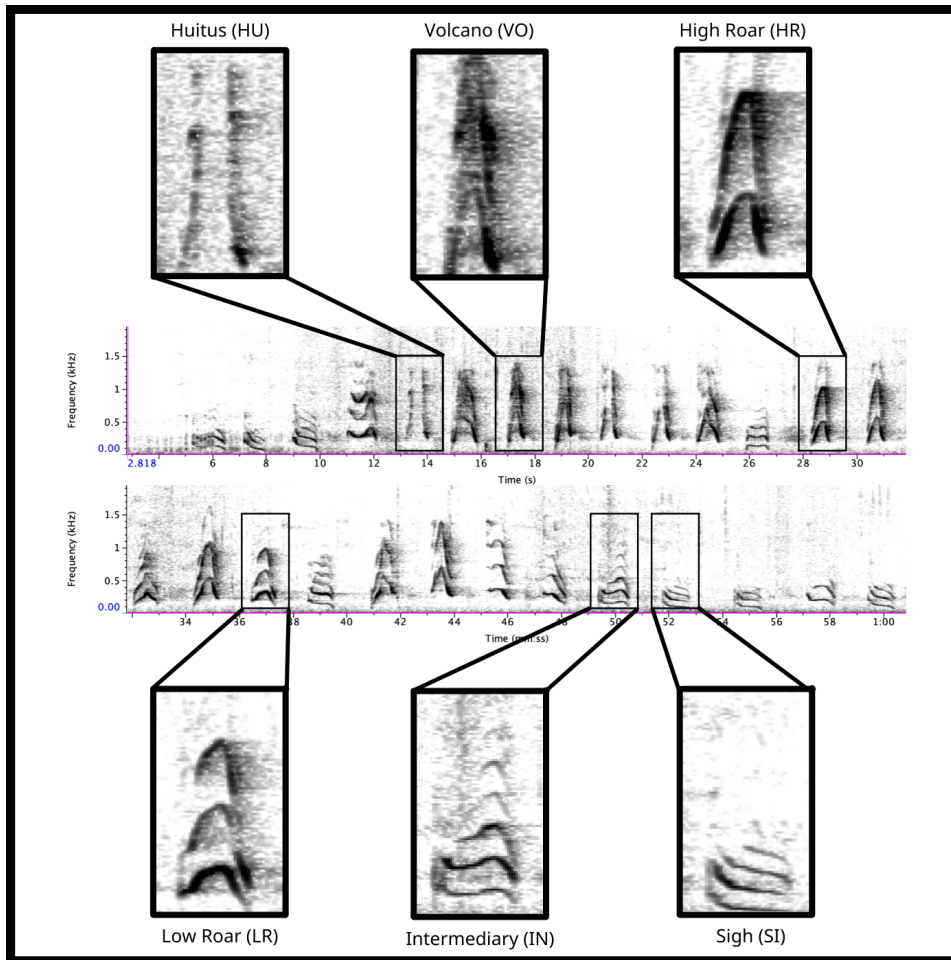
213 by drawing selections that tightly bounded the start and end of each pulse (Fig. S1) and assigned call  
214 type labels using the classification scheme outlined in Table 2. Except for huitus pulses (for which  
215 the rising and falling sounds are broken by silence), we operationally defined a pulse as the longest  
216 continuous sound produced on a single exhalation. Because most long calls are preceded and/or  
217 followed by a series of short bubbling sounds, we used a threshold duration of  $\geq 0.2$  seconds to  
218 differentiate pulses from these other sounds. Most selections were drawn with a fixed frequency  
219 range from 50 Hz to 1 kHz; however, in cases where the maximum fundamental frequency exceeded  
220 1 kHz (e.g., huitus and volcano roars), selections were drawn from 50 Hz to 1.5 kHz. Occasionally,  
221 we manually reduced the frequency range of selections if there were disturbing background sounds,  
222 but only if this did not affect measures of the fundamental frequency contour or high-energy  
223 harmonics. We noted whether selections were tonal (i.e., the fundamental frequency contour was  
224 fully or partially visible) and whether they contained disturbing background noises such as birds,  
225 insects, or breaking branches.

226 Our selected feature set comprised 25 extracted measurements made in Raven (Table S1) as  
227 well as an additional 19 measurements estimated using the R package *warbleR* (Araya-Salas & Smith-  
228 Vidaurre, 2017). Prior to analyzing sounds in *warbleR*, we filtered out all pulse selections that were  
229 atonal or contained disturbing background noise, resulting in 2,270 clips. Two additional  
230 measurements (minimum and maximum) of the fundamental frequency (F0) were made using the  
231 “freq\_ts” function in *warbleR* with the following settings: wavelength = 512, Hanning window, 70%  
232 overlap, 50 - 1,500 Hz, threshold = 85%. We then saved printed spectrograms depicting the F0  
233 contours for each. One observer (WME) visually screened the minimum and maximum values of  
234 the F0 contours and scored them as accurate or inaccurate. After removing those pulses for which  
235 one or both F0 measures were inaccurate, the final full dataset comprised 1,033 pulses from 117  
236 long calls for which all 46 parameters were measured.

237

## 238 **Audio-Visual Analysis**

239           To assess the inter-rater reliability (IRR) of the audio-visual analysis, we randomly selected  
240 300 pulses (saved as individual .wav files). We included this step to remove any bias that may be  
241 introduced by information about the position or sequence of a pulse-type within a long call. Using  
242 the spectrograms and descriptions of pulse types published by Spillmann and colleagues (Spillmann  
243 et al., 2010), three observers (WME, WR, HK) labeled each sound as one of six pulse types (Fig. 1).  
244 Prior to completing this exercise, all observers had at least six months' experience classifying pulse  
245 types, which involved routine feedback and three-way discussion. We used the R package *irr* (Gamer  
246 et al., 2012) to calculate Cohen's kappa (a common statistic for assessing IRR for categorical  
247 variables) for each pair of observers, and averaged these values to provide an overall estimate of IRR  
248 (Light's kappa) across all pulse types (cf. Hallgren, 2012; Light, 1971).



249

250 **Figure 1. Spectrogram depicting long call pulse types.** Pulses include HU = huitus, VO =  
251 volcano, HR = (high) roar, LR = low roar, IN = intermediary, SI = sigh. Spectrograms produced in  
252 Raven Pro 1.6.

253

## 254 **Supervised Classification**

255 For the supervised classification analysis, one observer (WME) manually classified all pulses  
256 (N=1,033). We then used support vector machines (SVM) in the R package *e1071* (Meyer et al.,  
257 2021) to evaluate how well pulse types could be discriminated using a supervised machine learning  
258 approach. SVMs are commonly used for supervised classification and have been successfully applied  
259 to the classification of primate calls (Clink & Klinck, 2020; Fedurek et al., 2016; Turesson et al.,

260 2016). We used the sigmoidal kernel as previous research using SVM has found the most robust  
261 results using this kernel type (Clink & Klinck, 2020) and we estimated the best values for the gamma  
262 and cost parameters using the “tune” function. Following this, we calculated our classification  
263 accuracy using 10 iterations of leave-one-out cross-validation. Lastly, we used SVM recursive feature  
264 elimination to rank variables in order of their importance for classifying call types (cf. Clink et al.,  
265 2018). For each of the top five most influential variables identified by recursive feature elimination,  
266 we used Kruskal-Wallis nonparametric tests due to the non-normal distribution of the residuals  
267 when applying linear models. We followed these with Dunn's test of multiple comparisons to  
268 examine differences among pulse types and unsupervised clusters (described below) – applying the  
269 Benjamini-Hochberg adjustment to control the false discovery rate – using the R package *FSA*  
270 (Ogle et al., 2022).

271

## 272 **Unsupervised Clustering**

273 For the unsupervised analysis, we used both hard- and soft-clustering approaches. For hard  
274 clustering, we used affinity propagation, which has the advantage that it does not require the user to  
275 identify the number of clusters a priori; further, because all data points are considered  
276 simultaneously, the results are not influenced by the selection of an initial set of points (Frey &  
277 Dueck, 2007). Using the R package *apcluster* (Bodenhofer et al., 2011), we systematically varied the  
278 value of ‘q’ in 0.25 increments from 0 to 1. By comparing the mean silhouette coefficient for each of  
279 the cluster solutions (Wang et al., 2008), we found that  $q = 0$  produced the optimal number of  
280 clusters and thus we report the results from this model. We used silhouette coefficients to quantify  
281 the stability of the resulting clusters (cf. Clink & Klinck, 2020).

282 For the soft clustering analysis, we used C-means fuzzy clustering. In this analysis, each pulse  
283 is assigned a membership value (m ranges from 0 = none to 1 = full accordance) for each of the



284 clusters. We first determined the optimal number of clusters ( $c$ ) by evaluating measures of internal  
285 validation and stability generated in the R package *cValid* (Brock et al., 2008) when  $c$  varied from 2  
286 (the minimum) to 7 (one more than the previously described number of pulse types). We then  
287 systematically varied the fuzziness parameter  $\mu$  from 1.1 to 5 (i.e., 1.1, 1.5, 2, 2.5, etc.: cf. Zhou et al.,  
288 2014)) using the R package ‘cluster’ (Maechler et al., 2021). When  $\mu = 1$ , clusters are tight and  
289 membership values are binary; however, as  $\mu$  increases, cases can show partial membership to  
290 multiple clusters, and the clusters themselves thereby become fuzzier and can eventually merge,  
291 leading to fewer clusters (Fischer et al., 2016). We used measures of internal validity (connectivity,  
292 silhouette width, and Dunn index) and stability (average proportion of non-overlap = APN, average  
293 distance = AD, average distance between means = ADM, and figure of merit = FOM) to evaluate  
294 the cluster solutions in the R package *cValid* (Brock et al., 2008). Once we had identified the best  
295 solution, we calculated typicality coefficients to assess the discreteness of each pulse, wherein higher  
296 values indicate pulses that are well separated from other clusters and lower values indicate pulses  
297 that are intermediate between classes (cf. Cusano et al., 2021; Wadewitz et al., 2015).

298         Non-linear dimensionality reduction techniques have recently emerged as fruitful  
299 alternatives to traditional linear techniques (e.g., principal component analysis) for classifying animal  
300 sounds (Sainburg et al., 2020). Uniform Manifold Approximation and Projection (UMAP) is a state-  
301 of-the-art unsupervised machine learning algorithm (McInnes et al., 2018) that has been applied to  
302 visualizing and quantifying structures in animal vocal repertoires (Sainburg et al., 2020). Like  
303 ISOMAP and t-SNE, UMAP constructs a topology of the data and projects that graph into a lower-  
304 dimensional embedding (McInnes et al., 2018; Sainburg et al., 2020) UMAP has been shown to  
305 preserve more global structure while achieving faster computation times (McInnes et al., 2018) and  
306 has been effectively applied to meaningful representations of acoustic diversity (reviewed in

307 Sainburg et al., 2020). This approach removes any a priori assumptions about which acoustical  
308 features are most salient or easily measured by humans.

309 We applied UMAP separately to the 46-feature set and to time-frequency representations of  
310 extracted pulses. In the latter case, we used as inputs power density spectrograms of 0.9-s duration  
311 audio clips centered at the temporal midpoint of annotated pulses. The chosen duration was fixed  
312 irrespective of the selection duration. This means that, for short selections, the spectrograms also  
313 included sounds outside of the original selection. Short-time Fourier transforms of the clips were  
314 computed, using SciPy's (<https://scipy.org/>) *spectrogram* function, with a Hann window of 50 ms and  
315 50% frame overlap (20 Hz frequency resolution, 25 ms time resolution). Spectral levels were  
316 converted to the decibel scale by applying  $10 \times \log_{10}$ . The bandwidth of the resulting spectrograms  
317 was limited to 50-1000 Hz prior to UMAP computation to suppress the influence of low-frequency  
318 noise on clustering. We used the *UMAP* function from the Python package *umap-learn* (McInnes et  
319 al., 2018) to compute the low-dimensional embeddings. Finally, we calculated Hopkin's statistic of  
320 clusterability on the resultant UMAP using the R package *factoextra* (Kassambara & Mundt, 2020).

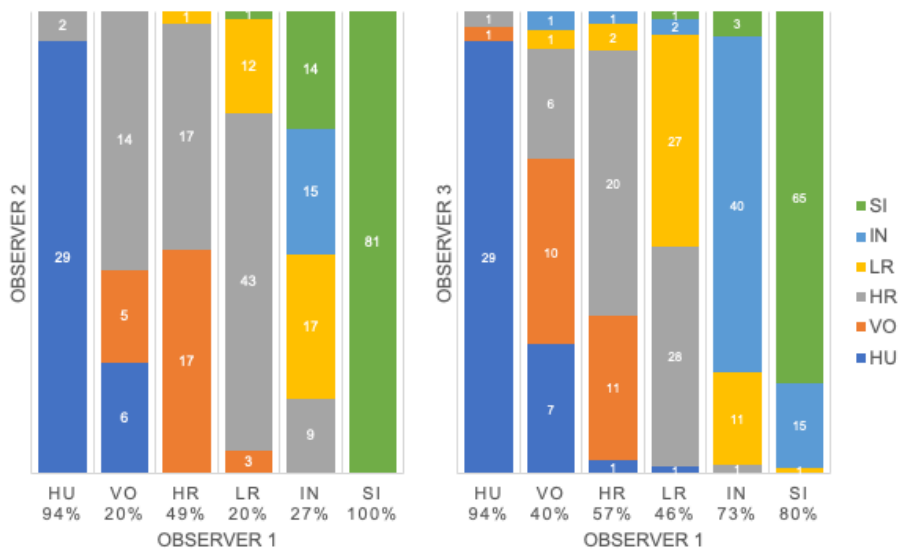
321 Finally, we reviewed the outputs of our unsupervised clustering approaches to assess the  
322 putative number of pulses and graded variants. To identify a simple, data-driven, repeatable method  
323 for manually classifying pulse types, we began by pooling the typical pulses that belonged to each of  
324 the clusters identified by fuzzy clustering. Because F0 is a highly salient feature in long call  
325 spectrograms, our approach focused on the shape and height (or maximum frequency) of this  
326 feature. Using our revised definitions, we repeated the 1) audio-visual analysis and calculated IRR  
327 using manual labels from the same 300 pulses reviewed by the same three observers as before, and  
328 2) SVM classification of 500 randomly selected pulses scored by a single observer (WME) following  
329 the methods described above.

330

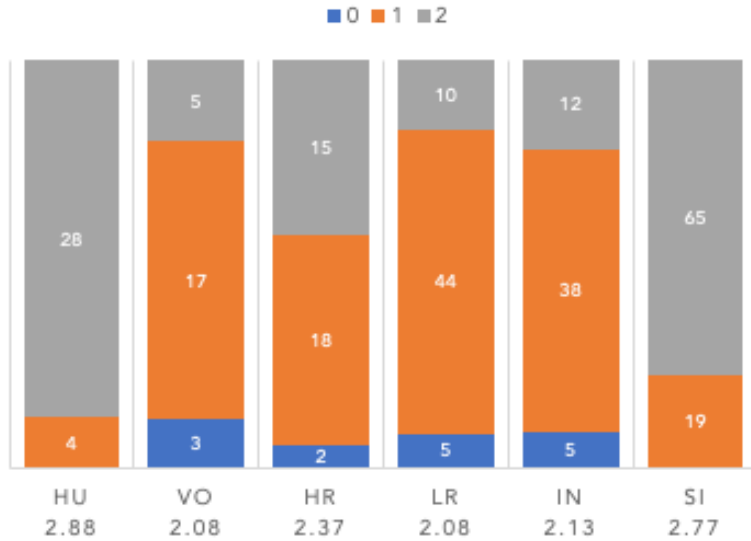
## 331 RESULTS

### 332 Audio-visual analysis

333 Based on manual labels from three observers using audio-visual classification methods, we  
334 calculated Light's kappa  $\kappa = 0.599$  (i.e., the arithmetic mean of Cohen's Kappa for observers 1-2 =  
335 0.48, 1-3 = 0.60, and 2-3 = 0.60), which indicated only moderate agreement among observers  
336 (Landis & Koch, 1977). Classification agreement varied widely by pulse type (Fig. 2, Table 3).  
337 Whereas hutilus and sigh pulse types showed high agreement among observers (mean 2.88 and 2.77,  
338 respectively, where 3 indicates full agreement), low roar and volcano pulse types showed very low  
339 agreement (mean 2.08).



340



341  
 342 **Figure 2. Audio-visual classification agreement across observers.** Stacked barplots indicating  
 343 (top) classification agreement by pulse type between observer 1-2 and observer 1-3 and (bottom) the  
 344 number of observers who agreed on the pulse types assigned by observer 1; the average agreement  
 345 index is indicated below each pulse type and demonstrates high agreement for HU and SI ( $\geq 2.77$ ),  
 346 but low agreement for VO and LR (2.08).

347  
 348 **Table 3.** Mean values for A/V agreement index, SVM pulse classification accuracy, typicality  
 349 coefficient, and frequency measures by pulse type.

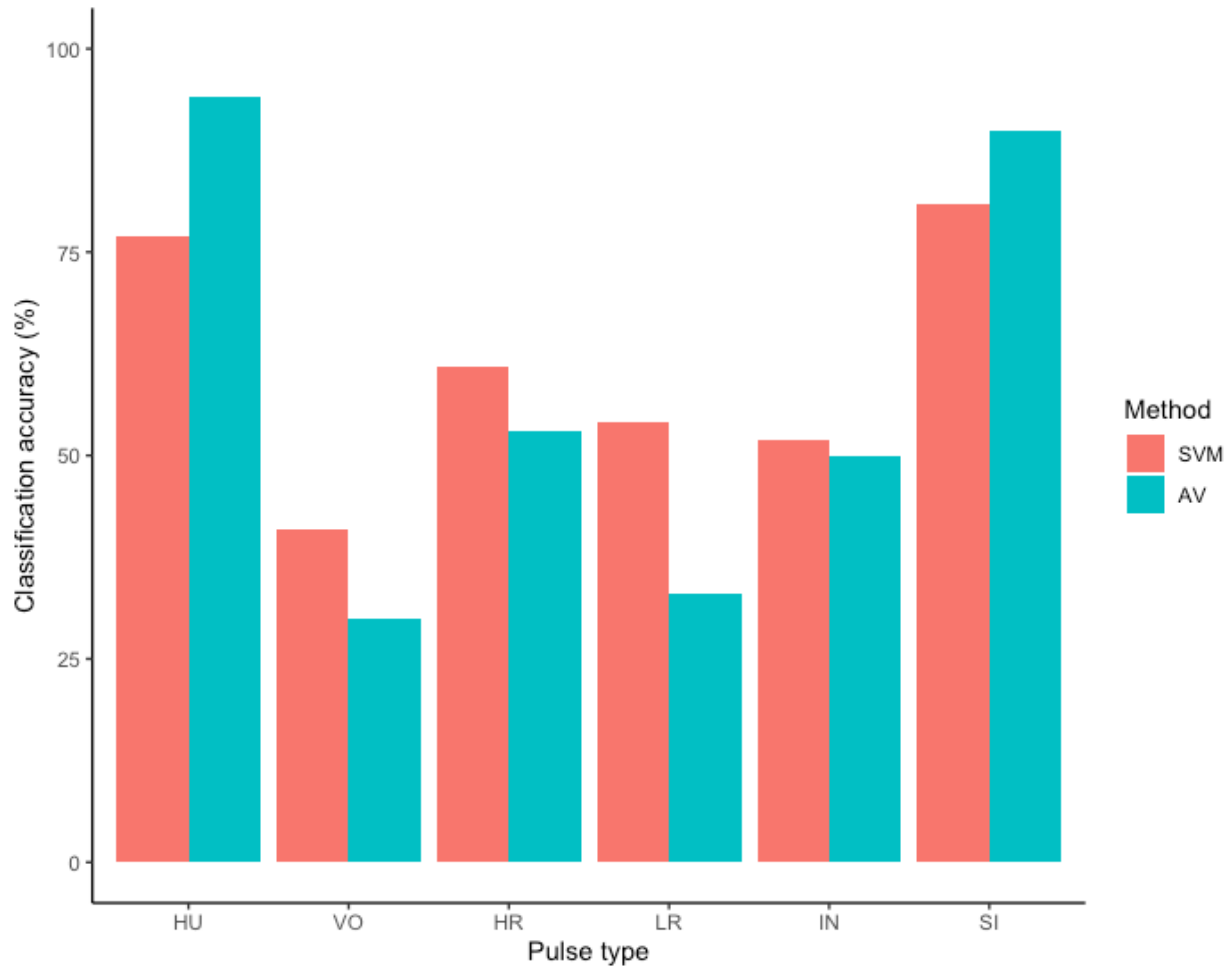
Pulse	A/V index	SVM	Typicality	Center	Peak	Mean peak	3rd quart	1st quart
HU	2.88	77%	0.90	443.3	421.0	436.4	585.3	370.3
VO	2.08	41%	0.98	483.1	442.3	505.6	592.6	376.7
HR	2.37	61%	0.94	440.0	409.9	450.1	533.8	358.7
LR	2.08	54%	0.81	266.3	252.2	271.8	312.0	231.4
IN	2.13	52%	0.84	249.7	242.7	244.6	288.8	225.5
SI	2.77	81%	0.97	203.0	201.1	194.6	239.1	172.5

350  
 351  
 352

353 **Supervised classification using extracted feature set: support vector machines**

354 We tested the performance of SVM for the classification of orangutan long call pulse types  
355 using our full acoustic feature dataset. Using leave-one-out cross-validation, we found the average  
356 classification accuracy of pulse types was 64.8% (range: 64.28 – 65.44  $\pm$  0.10 SE). SVM classification  
357 accuracy was higher than IRR agreement scores for most pulse types, though human observers were  
358 better at discriminating huitsus and sigh pulses (Fig. 3). Classification accuracy was highly variable  
359 across pulse types. Whereas sighs and huitsuses were classified with the highest accuracy (81 and  
360 77%, respectively), volcanoes were classified with the lowest accuracy (41%: Fig. 3, Table 3).

361 Recursive feature elimination revealed that center frequency, peak frequency, mean peak  
362 frequency, and third and first frequency quartiles were the most influential variables (Table 3). In all  
363 five influential features, high roars, huitsuses, and volcanoes overlapped, and in four of five features,  
364 intermediaries overlapped low roars (Fig. S2, Table S2). All other pairwise comparisons of pulse  
365 types showed significant differences in all features.



366

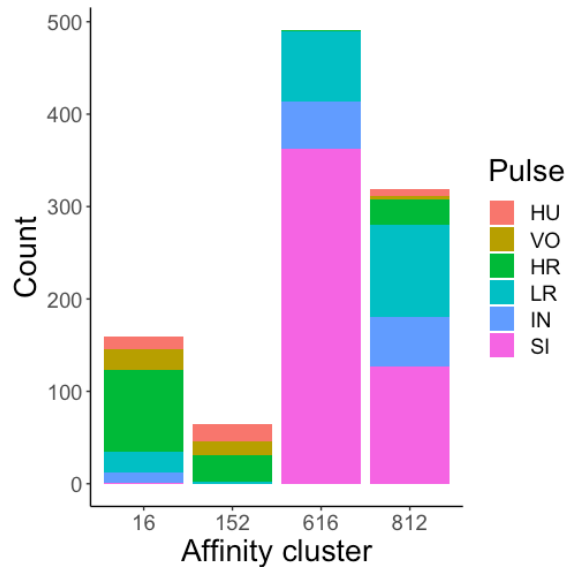
367 **Figure 3. Barplot of classification accuracy for original pulse scheme.** Comparison of  
368 classification accuracy of audio-visual classification (AV), calculated as the average agreement  
369 between three observer pairs compared to supervised machine learning classification (SVM).

370

### 371 **Unsupervised clustering using extracted feature set: hard and soft clustering**

372 Affinity propagation resulted in four clusters with an average silhouette coefficient of 0.32  
373 (range: -0.22 – 0.61). Of these four clusters, two (clusters 616 and 152: Fig. 4) had relatively high  
374 silhouette coefficients (0.45 and 0.29, respectively) and separated the higher-frequency pulses (i.e.,  
375 HU, VO, and HR pulses) from lower-frequency ones (i.e., LR, IN, and SI). The remaining two  
376 clusters had low silhouette coefficients (cluster 16 = 0.19, cluster 812 = 0.21) and both contained

377 calls from all six pulse types (Fig. 4). We analyzed the separation of unsupervised clusters using the  
378 influential features identified from recursive feature elimination (Fig. S2). Two of the four clusters  
379 (16 and 152) overlapped in four of five features. These clusters primarily comprised high roars,  
380 volcanoes, and huituses.  
381



382  
383 **Figure 4. Stacked barplots of affinity propagation clusters** showing the number of calls in each  
384 cluster classified by pulse type.

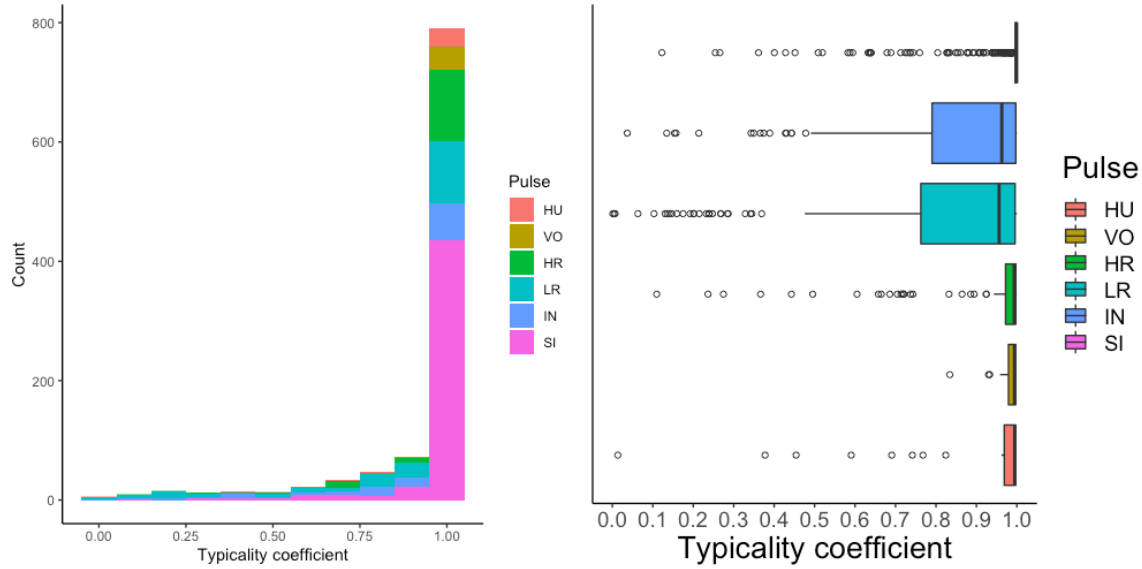
385  
386 In a final approach to clustering our extracted feature set, we used c-means fuzzy clustering  
387 to provide another estimate of the number of clusters in our dataset and quantify the degree of  
388 gradation across pulse types. All three internal validity measures (connectivity, Dunn, and silhouette)  
389 and three of four stability measures (APN, AD, and ADM) indicated that the two-cluster solution  
390 was optimal. Only FOM indicated a 3-cluster solution was marginally more stable (0.855 for 2 vs.  
391 0.860 for 3 clusters). We found that  $\mu = 1.1$  yielded the highest average silhouette width (0.312);  
392 silhouette widths decreased as  $\mu$  increased.

393 Typicality coefficients were high overall (mean:  $0.92 \pm 0.006$  SE, Fig. 5) but varied widely by  
394 pulse type. Whereas volcanoes and sighs had the highest typicality coefficients (0.98 and 0.97,  
395 respectively) and intermediaries and low roars had the lowest coefficients (0.84 and 0.81,  
396 respectively, Table 3). Pairwise comparisons of typicality coefficients showed that typicality  
397 coefficients for low roars and intermediaries were significantly lower than those of all other pulse  
398 types but did not significantly differ between these two pulses (Fig. S2, Table S2).

399 We determined the thresholds for typical ( $>0.976$ ) and atypical calls ( $<0.855$ ) (cf. Wadewitz  
400 et al., 2015). Overall, 69% of calls were ‘typical’ for their cluster and 17% were ‘atypical’; however,  
401 pulse types varied greatly (Fig. 6). Whereas sighs and volcanoes had a high proportion of typical calls  
402 (85% and 80% respectively), low roars and intermediaries had a high proportion of atypical calls  
403 (44% and 40% respectively).

404 Typical calls were found in both clusters (Fig. 6). Typical calls in cluster one included high  
405 roars, huituses, low roars, and volcanoes and those in cluster two included sighs, low roars, and  
406 intermediaries. Whereas typical sighs, huituses, and volcanoes were found in only one cluster (and  
407 only 1-2 intermediaries and high roars were typical for a secondary cluster), 24% of low roars  
408 belonged to a secondary cluster. Overall, cluster one comprised 189 typical and 99 atypical calls  
409 (53% and 28% of 353 calls, respectively) and cluster two comprised 526 typical and 75 atypical calls  
410 (77% and 11% of 680 calls, respectively), indicating that calls in cluster two were better separated  
411 from other call types than those in cluster one. We compared typical calls in each cluster and found  
412 that calls in different clusters significantly differed from each other in all five influential features (Fig.  
413 S2, Table S2a).



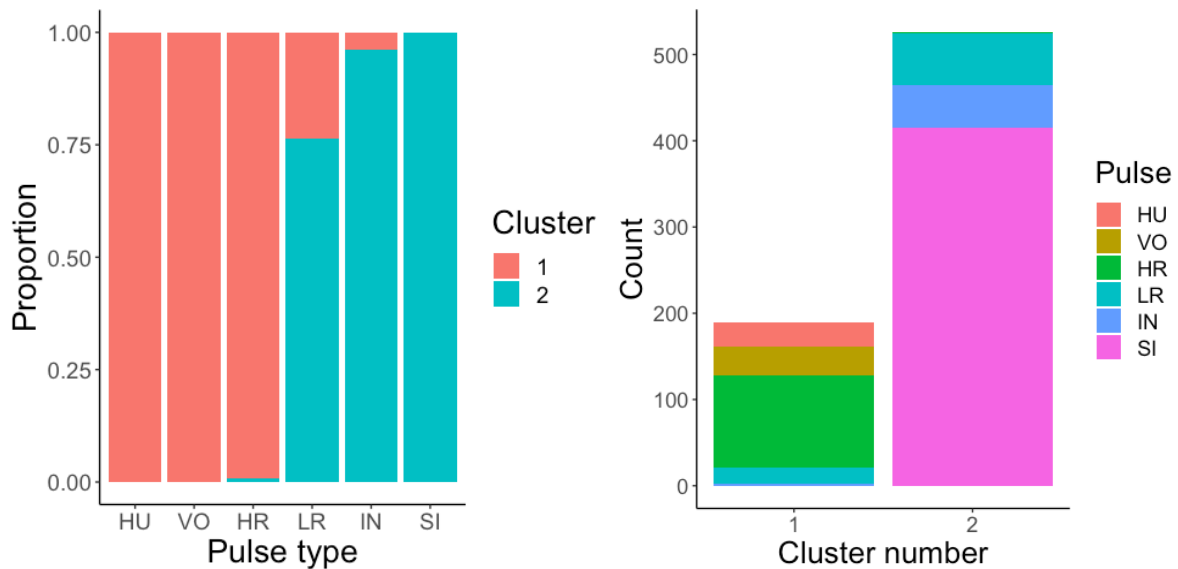


414

415 **Figure 5. Typicality coefficients for each pulse type** a) Histogram showing the distribution of  
416 coefficients and b) boxplot showing typicality values for each pulse type. Typicality thresholds were  
417 calculated following (Wadewitz et al., 2015). Typical calls were those whose typicality coefficients  
418 exceeded 0.976 and atypical calls were those below 0.855.

419

420



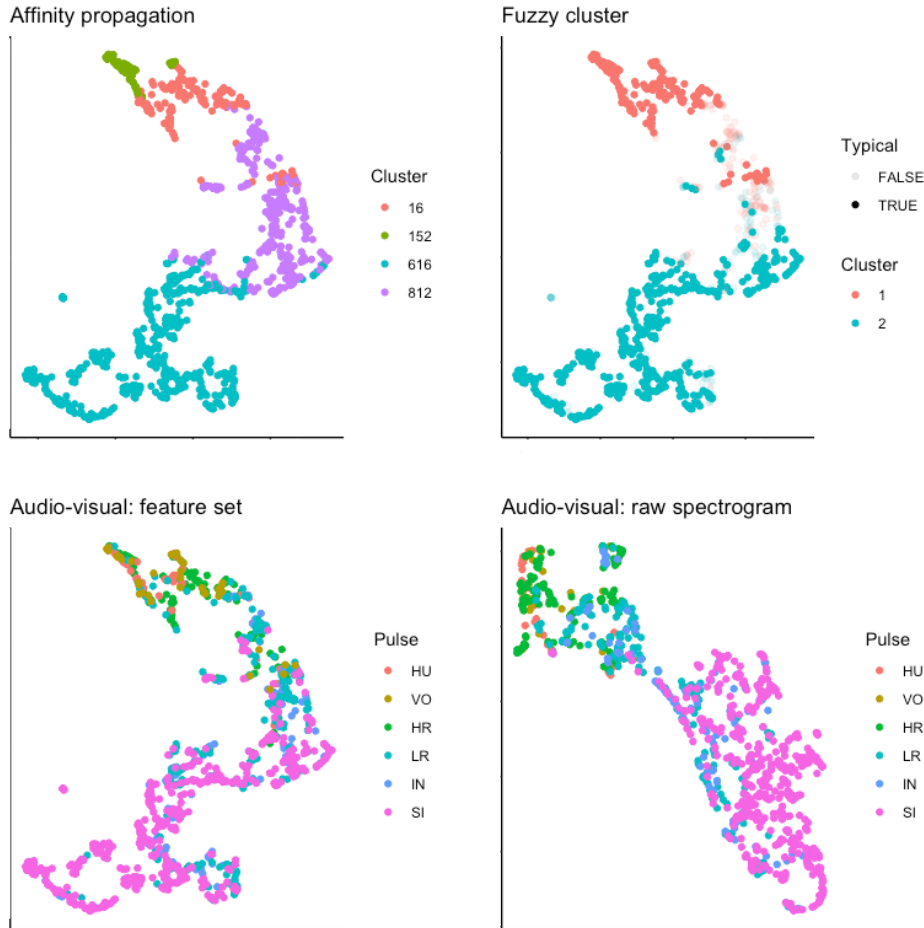
421

422 **Figure 6. Stacked barplots of typical calls** a) the proportion of each pulse type that was typical  
423 for each cluster and b) the number of typical calls in each cluster classified by pulse type.

424

#### 425 **UMAP visualization of extracted features and spectrograms**

426 We used UMAP to visualize the separation of individual pulses using our extracted feature  
427 set, comparing the cluster results from affinity propagation and fuzzy clustering with manual  
428 classification (Fig. 7). We also used UMAP to visualize the separation of pulses based on the power  
429 density spectrograms (Fig. 7). For both datasets, it appears that there are two loose and incompletely  
430 separated clusters as well as a smaller number of pulses that grade continuously between the two  
431 clusters. The Hopkins statistic of clusterability for the extracted feature set was 0.940 and 0.957 for  
432 the power spectrograms, both of which indicate strong clusterability of calls.



433

434 **Figure 7. UMAP projection of 46-feature dataset.** Colors indicate four clusters identified using  
435 unsupervised affinity propagation (upper left), two clusters and typical calls identified by fuzzy  
436 clustering (upper right), six pulse types labeled by human observer using the extracted feature set  
437 (lower left), and raw power density spectrograms (lower right).

438

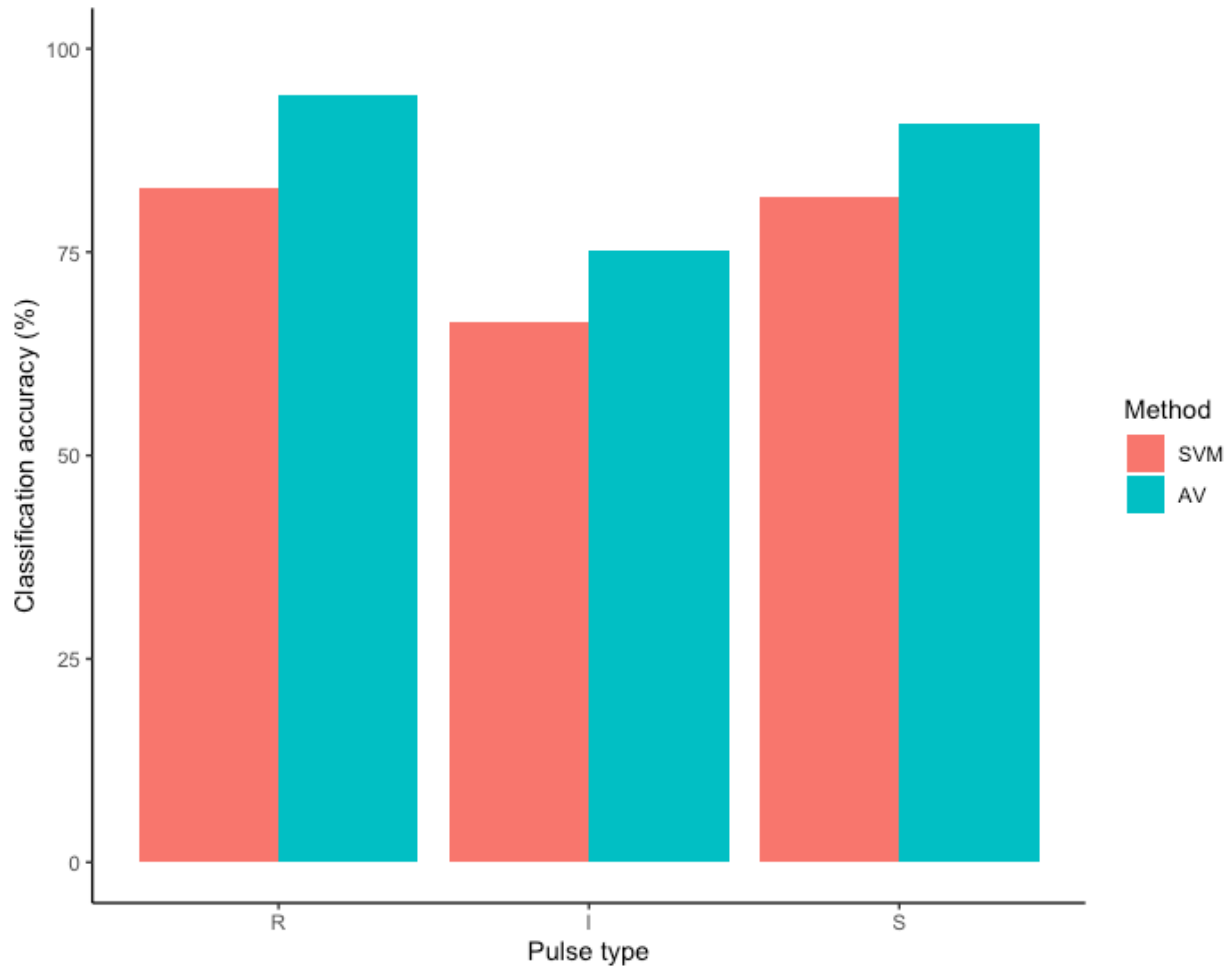
### 439 Identification and evaluation of a new classification scheme

440 Collectively, our unsupervised clustering approaches showed broad agreement for a two-  
441 cluster solution with graded pulses occurring along a spectrum between the two classes. In fuzzy  
442 typical cluster 1, the mean value for F0 max was  $764.3 \text{ Hz} \pm 351.5 \text{ SD Hz}$  (range = 320-1,500);  
443 whereas for those pulses belonging to fuzzy typical cluster 2, the mean value of F0 max was  $225.3 \pm$

444 SD 67.9 SD Hz (range = 80-440). Pulses that were not typical for either cluster had a mean F0 max  
445 of  $345.8 \pm 159.9$  SD Hz. Based on these patterns, as well as the shape of the F0 (a feature that was  
446 commonly used to distinguish among pulse types in previous studies), we distinguished among  
447 pulses as follows: **Roar (R)** = F0 ascends and reaches its maximum ( $>350$  Hz) at or near the  
448 midpoint of the pulse before descending, **Sigh (S)** = F0 descends and reaches its maximum  
449 (typically, but not always  $< 350$  Hz) at start of the pulse (i.e., no ascending portion of F0), and  
450 **Intermediate (I)** = either a) maximum F0 value occurs at the start of the pulse but with an  
451 ascending portion later in pulse, or b) F0 ascends and reaches its maximum ( $<350$  Hz) at or near the  
452 midpoint of the pulse.

453       These revised definitions yielded Light's kappa  $\kappa = 0.838$  (i.e., the arithmetic mean of  
454 Cohen's Kappa for observers 1-2 = 0.84, 1-3 = 0.86, and 2-3 = 0.78), indicating near-perfect  
455 agreement among observers (Landis & Koch, 1977). Classification agreement varied only slightly by  
456 pulse type, with roars showing the highest agreement among observers (mean 2.92, where 3  
457 indicates full agreement), and intermediaries and sighs showing slightly lower agreement (mean 2.79  
458 and 2.72, respectively). Using leave-one-out cross-validation, we found the average classification  
459 accuracy of pulse types using SVM was 82.1% (range: 80.8 – 85.0  $\pm$  0.47 SE). SVM classification  
460 accuracy was lower than IRR agreement scores for most pulse types (Fig. 8) but both roars and sighs  
461 were classified with high agreement using both methods.

462



463

464 **Figure 8. Barplot of classification accuracy for revised pulse scheme.** Comparison of  
465 classification accuracy of audio-visual classification (AV), calculated as the average agreement  
466 between three observer pairs compared to supervised machine learning classification (SVM).

467

## 468 **DISCUSSION**

469 Here we present an extensive qualitative and quantitative assessment of the vocal complexity  
470 of the long-call vocalizations of Bornean orangutans. Relying on a large dataset comprising 46  
471 acoustic measurements from 1,033 pulses from 117 long calls recorded from 13 males, we compared  
472 the ability of human observers and supervised and unsupervised machine-learning techniques to  
473 discriminate unique call (or pulse) types. Three human observers performed relatively well at

474 discriminating two pulse types – huitus and sigh – but our inter-rater reliability score (i.e., Light’s  
475 kappa) showed only moderate agreement across the six pulse types. Although support vector  
476 machines (SVM) performed better than human observers in classifying most pulse types (except for  
477 huitus and sigh pulses), the overall accuracy was less than 65%. Like humans, SVM’s were best at  
478 discriminating huitus and sigh pulse types but performed relatively poorly for the others. Poor  
479 classification accuracy across audio-visual and supervised machine learning approaches indicates that  
480 these six pulse types are not discrete. This finding suggests that attempting comparisons of different  
481 pulse types (cf. Davila Ross & Geissmann, 2007; Spillmann et al., 2010) across observers or studies  
482 is not advisable, since these classes are not reliably reproduced by different observers or well  
483 separated by a robust set of acoustic features.

484       Having demonstrated that these six pulse types were not well discriminated, we turned to  
485 unsupervised clustering to characterize and classify the diversity of pulses comprising orangutan long  
486 calls. Whereas hard clustering, such as affinity propagation, seeks to identify a set of high-quality  
487 exemplars and corresponding clusters (Frey & Dueck, 2007), soft, or fuzzy, clustering is an  
488 alternative or complementary approach to evaluate and quantify the discreteness of call types within  
489 a graded repertoire (Cusano et al., 2021; Fischer et al., 2016; Wadewitz et al., 2015). Although the  
490 hard and soft unsupervised techniques yielded different clustering solutions – four clusters for  
491 affinity propagation and two for fuzzy c-means – both methods showed relatively poor separation  
492 across pulse types. Importantly, both hard and soft clustering solutions separated high-frequency  
493 pulses (i.e., HU, VO, and HR) from low-frequency ones (i.e., LR, IN, SI), but low roars and  
494 intermediaries showed low typicality coefficients and occurred in both fuzzy clusters. Together, the  
495 results of unsupervised clustering support our interpretation of the manual and supervised  
496 classification analysis in demonstrating that orangutan long calls contain a mixture of discrete and  
497 graded pulse types.

498 We used a final approach, UMAP, to visualize the separation and quantify the clusterability  
499 of call types. Because the number and type of features selected can have a strong influence on the  
500 cluster solutions and their interpretations (Fischer et al., 2016; Wadewitz et al., 2015), we compared  
501 the results of our extracted 46-feature dataset with raw power density spectrograms as inputs. Both  
502 datasets yielded similar and high Hopkin's statistic values, indicating strong clusterability of calls. At  
503 the same time, both datasets generated a V-shaped cloud of points showing two large loose clusters  
504 with a spectrum of points lying along a continuum between them.

505 Based on our comprehensive evaluation of orangutan pulse types, we have proposed a  
506 revised approach to the classification of orangutan pulses that we hope provides improved  
507 reproducibility for future researchers. We recommend using the following terms to categorize the  
508 range of pulse types comprising orangutan long calls: 1) 'Roar' for high-frequency pulses, 2) 'Sigh'  
509 for low-frequency pulses, and 3) 'Intermediate' for graded pulses that fall between these two  
510 extremes. We have provided detailed descriptions of each of these pulse types and demonstrated  
511 that they can be easily and reliably identified among different observers and exhibit high  
512 classification accuracy using SVM.

513 Thus, we find that orangutan calls can be clustered into three pulse types (two discrete and  
514 one graded). The low diversity of call types suggests that these vocalizations are not particularly  
515 complex. Like the long-calls of other apes (chimpanzees, *Pan troglodytes schweinfurthii*: Arcadi, 1996;  
516 Marler & Hobbett, 1975; gibbons, *Hylobates* spp: Marshall & Marshall, 1976), orangutan long calls  
517 typically comprise an intro and/or build-up phase (quiet, staccato grumbles, not analyzed in the  
518 present study), climax (high-energy, high-frequency roars), and a let-down phase (low-energy sighs).  
519 The low number of discrete pulse types could be interpreted as support for the hypothesis that long-  
520 distance signals have been selected to facilitate signal recognition in dense and noisy habitats (Marler

521 et al., 1975). Yet, there is a spectrum of intermediate call types that yield a continuous gradation of  
522 sounds across phases and pulses, that seems to greatly boost the complexity of this signal.

523         Unfortunately, only a handful of studies have quantified the gradedness of animal vocal  
524 systems (but see Cusano et al., 2021; Fischer et al., 2017; Taylor et al., 2021; Wadewitz et al., 2015).  
525 Consequently, we are still lacking a comprehensive framework through which to quantify and  
526 interpret vocal complexity vis-à-vis graded repertoires (Fischer et al., 2017). Future research will  
527 explore the production of graded call types across individuals and call types to examine the sources  
528 of variation and the potential role of graded call types in orangutan communication.

529         In summary, we evaluated a range of supervised and unsupervised approaches to classifying  
530 and clustering sounds in animal vocal repertoires. We used a combination of traditional audio-visual  
531 methods and modern machine learning techniques that relied on human eyes and ears, a set of 46  
532 features measured from spectrograms, and raw power density spectrograms to triangulate diverse  
533 datasets and methods to answer a simple question: how many pulse types exist within orangutan  
534 long calls, how can they be distinguished, and how graded are they? While each approach has its  
535 strengths and limitations, taken together, they can lead to a more holistic understanding of call types  
536 within graded repertoires and contribute to a growing body of literature documenting the graded  
537 nature of animal communication systems.



539 **Table S1.** Table describing features measured in Raven Pro and warbleR (Specan and freq\_ts)

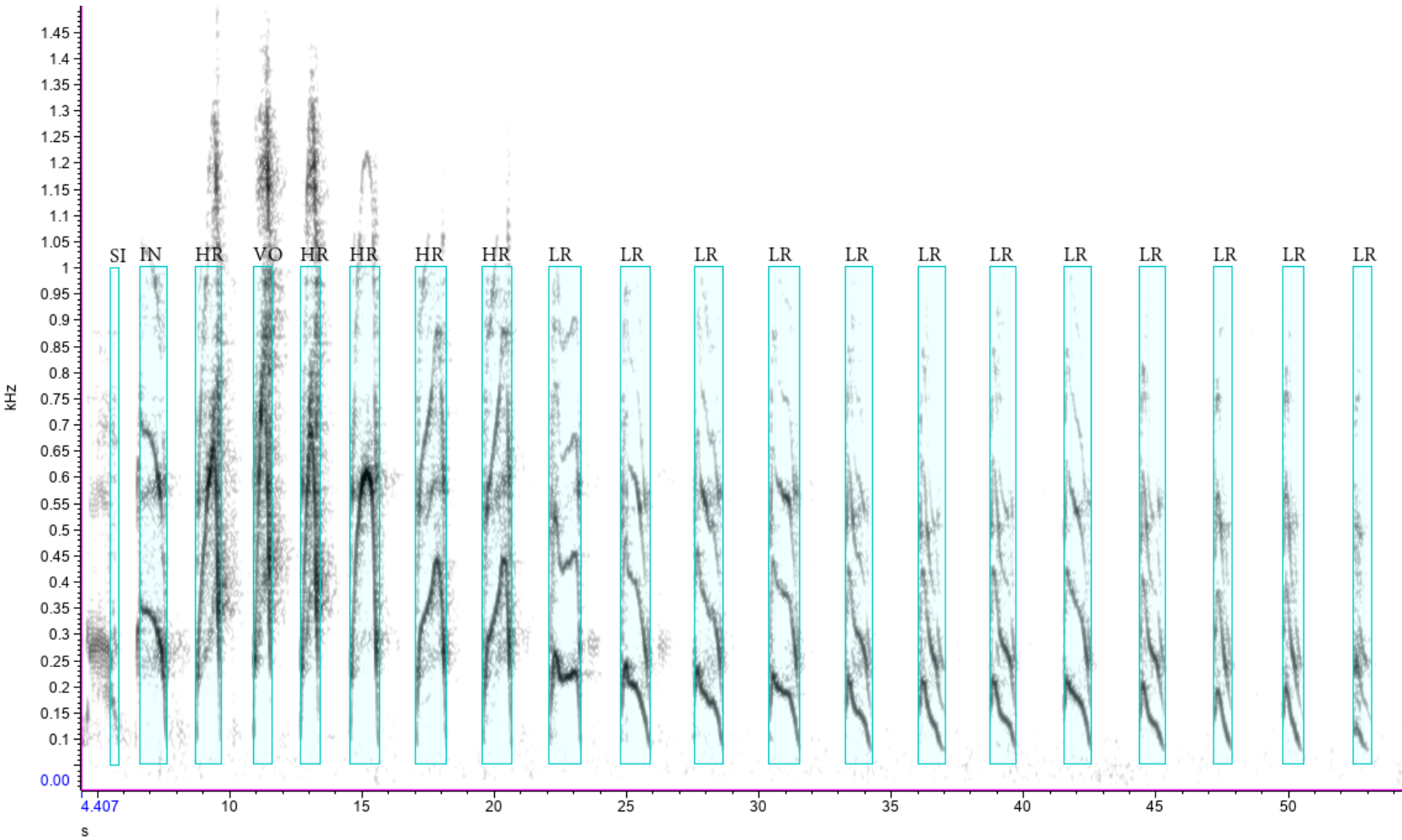
No	Program	Feature	Description
1	Raven	Delta.Time.s	difference between Begin Time and End Time for the selection (s)
2	Raven	Freq.5%.Hz	frequency at which summed energy exceeds 5% of total energy
3	Raven	Freq.95%.Hz	frequency at which summed energy exceeds 95% of total energy
4	Raven	Agg.Entropy.bits	aggregate entropy measures the disorder in a sound by analyzing the energy distribution (pure tone ~ 0)
5	Raven	Avg.Entropy.bits	average entropy measurement describes the amount of disorder for a typical spectrum within the selection
6	Raven	BW.50%	difference between the 25% and 75% frequencies (Hz)
7	Raven	BW.90%	difference between the 5% and 95% frequencies (Hz)
8	Raven	Center.Freq	frequency that divides the selection into two frequency intervals of equal energy (Hz)
9	Raven	Center.Time.Rel.	proportion of selection at which 50% of the sound energy has an earlier time
10	Raven	Dur.50%	difference between the 25% and 75% times (s)
11	Raven	Dur.90%	difference between the 5% and 95% times (s)
12	Raven	Freq.25%	frequency at which summed energy exceeds 25% of total energy (Hz)
13	Raven	Freq.75%	frequency at which summed energy exceeds 75% of total energy (Hz)
14	Raven	Peak.Freq	frequency at which Peak Power occurs within the selection (Hz)
15	Raven	PFC.Avg.Slope	Mean of the Peak Frequency Contour Slope Series of numbers (Hz/ms)
16	Raven	PFC.Max.Freq	Maximum of the Peak Frequency Contour Series of numbers (Hz)
17	Raven	PFC.Max.Slope	Maximum of the Peak Frequency Contour Slope Series of numbers (Hz/ms)
18	Raven	PFC.Min.Freq	Minimum of the Peak Frequency Contour Series of numbers (Hz)
19	Raven	PFC.Min.Slope	Minimum of the Peak Frequency Contour Slope Series of numbers (Hz/ms)
20	Raven	PFC.Num.Inf.Pts	Number of times the slope changes sign in Peak Frequency Contour Slope Series of numbers
21	Raven	Peak.Time.Rel.	proportion of selection at first time in a selection at which amplitude equal to Peak Amplitude occurs
22	Raven	Time.25%.Rel.	proportion of selection at which 25% of the sound energy has an earlier time
23	Raven	Time.5%.Rel.	proportion of selection at which 5% of the sound energy has an earlier time
24	Raven	Time.75%.Rel.	proportion of selection at which 75% of the sound energy has an earlier time

25	Raven	Time.95%.Rel.	proportion of selection at which 95% of the sound energy has an earlier time
26	specan	meanfreq	mean of frequency spectrum (kHz)
27	specan	sd	standard deviation of frequency (kHz)
28	specan	skew	skewness: asymmetry of the spectrum
29	specan	kurt	kurtosis: peakedness of the spectrum
30	specan	sp.ent	energy distribution of the frequency spectrum (pure tone ~ 0)
31	specan	time.ent	energy distribution on the time envelope (pure tone ~ 0)
32	specan	entropy	spectrographic entropy: product of time x spectral entropy
33	specan	sfm	spectral flatness (pure tone ~ 0)
34	specan	meandom	average of dominant frequency measured across the acoustic signal
35	specan	mindom	minimum of dominant frequency measured across the acoustic signal
36	specan	maxdom	maximum of dominant frequency measured across the acoustic signal
37	specan	dfrange	range of dominant frequency measured across the acoustic signal
38	specan	modindx	modulation index: cumulative difference between adjacent dominant frequencies / dominant frequency range
39	specan	startdom	dominant frequency measurement at the start of the signal
40	specan	enddom	dominant frequency measurement at the end of the signal
41	specan	dfslope	slope of the change in dominant frequency through time
42	specan	meanpeakf	frequency with highest energy from the mean frequency spectrum
43	specan	Freq_IQR	interquartile frequency range. Frequency range between 'freq.Q25' and 'freq.Q75' (kHz)
44	specan	Time_IQR	interquartile time range. Time range between 'time.Q25' and 'time.Q75' (s)
45	freq_ts	F0_min	frequency at which F0 contour is at its minimum value (kHz)
46	freq_ts	F0_max	frequency at which F0 contour reaches its maximum value (kHz)

540

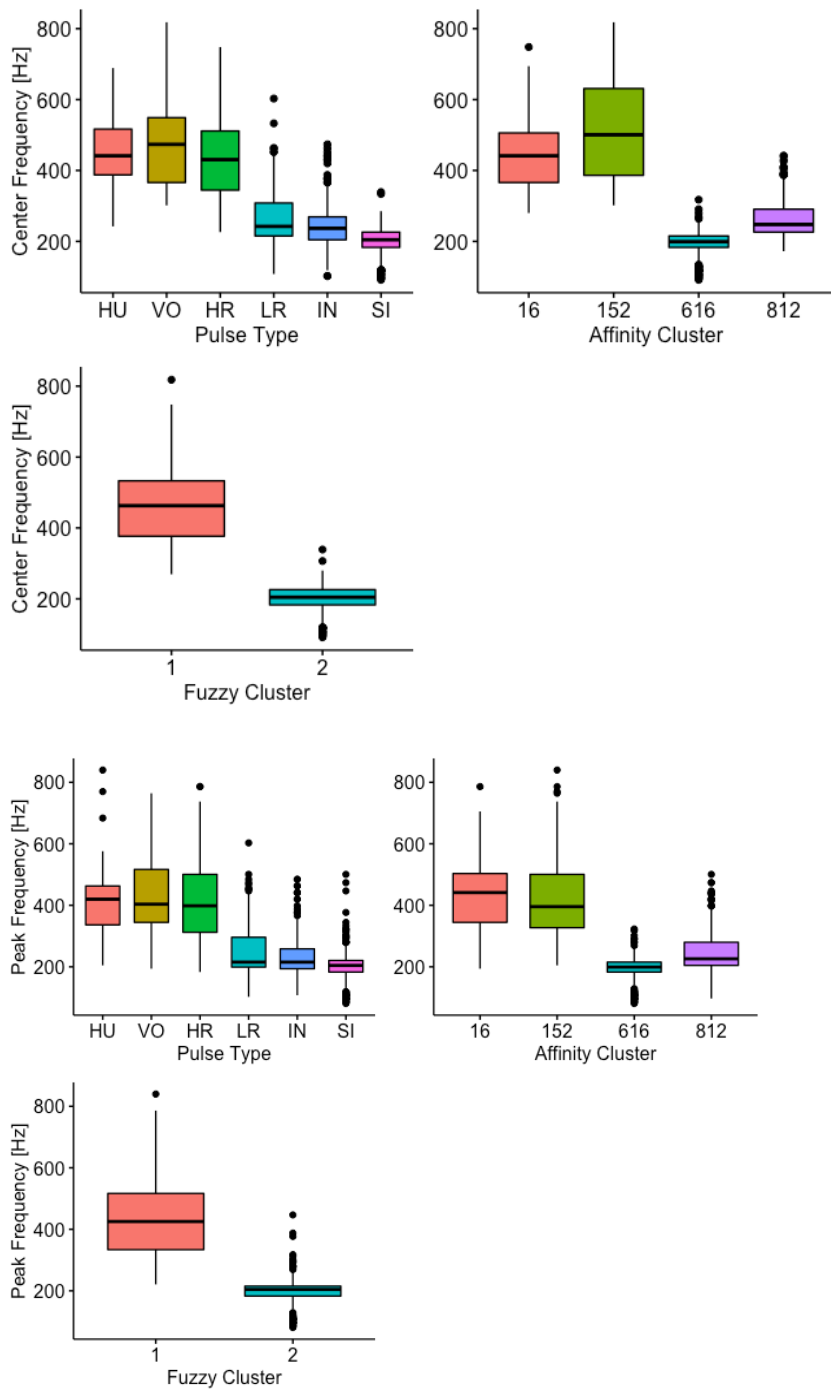
541

542 **Figure S1.** Example of annotated spectrogram



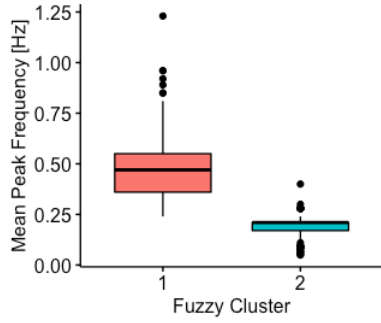
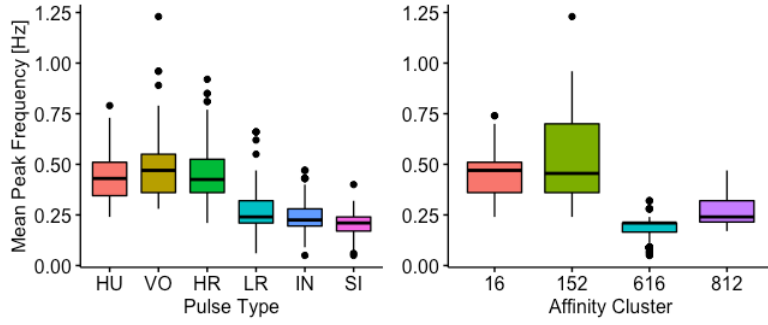
543

544 **Figure S2.** Boxplots of features that differed across human-labeled pulses (upper left), affinity  
545 propagation clusters (upper right), and typical calls in fuzzy clusters (lower left) for each of the  
546 following influential features: a) center frequency, b) peak frequency, c) mean peak frequency, d)  
547 third quartile frequency, e) first quartile frequency.

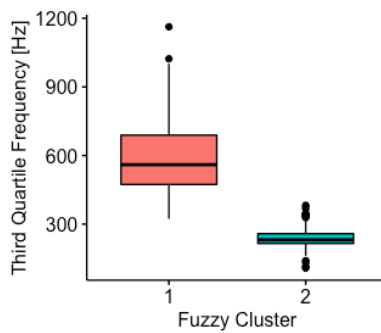
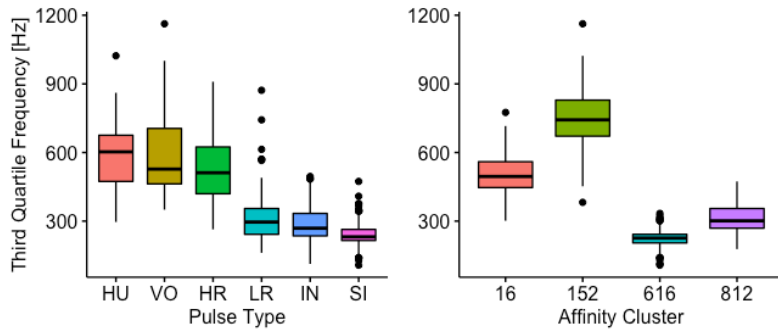


548

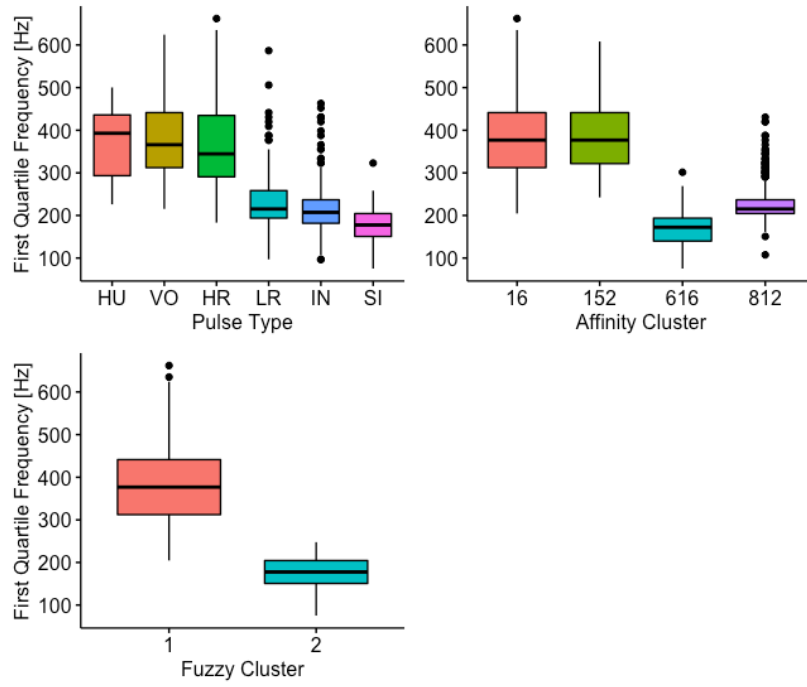
549



550



551



552

553 **Table S2a.** Table summarizing results of Kruskal-Wallis tests for differences among pulses or clusters identified by human observers,  
 554 affinity propagation, and fuzzy clustering for each of the top five influential variables.

Variable	A/V			AFFINITY			FUZZY		
	$\chi^2$	df	p	$\chi^2$	df	p	$\chi^2$	df	p
Center	557.81	5.00	0.00	738.53	3.00	0.00	417.16	1.00	0.00
Peak	425.31	5.00	0.00	588.78	3.00	0.00	406.49	1.00	0.00
Mean peak	528.18	5.00	0.00	677.78	3.00	0.00	421.95	1.00	0.00
Third quart	570.30	5.00	0.00	777.79	3.00	0.00	416.69	1.00	0.00
First quart	536.72	5.00	0.00	684.50	3.00	0.00	414.47	1.00	0.00

555

556 **Table S2b.** Table summarizing results of Dunn tests for pair-wise differences among pulses identified by human observers for each of the  
 557 top five influential variables.

A/V Pair	Center			Peak			Mean peak			Third quart			First quart		
	Z	P.unadj	P.adj	Z	P.unadj	P.adj	Z	P.unadj	P.adj	Z	P.unadj	P.adj	Z	P.unadj	P.adj
HR-HU	-0.21	0.84	0.84	-0.54	0.59	0.63	0.12	0.90	0.90	-0.60	0.55	0.64	-0.54	0.59	0.68
HR-IN	10.29	0.00	0.00	9.12	0.00	0.00	10.59	0.00	0.00	10.52	0.00	0.00	9.04	0.00	0.00
HR-LR	9.80	0.00	0.00	9.81	0.00	0.00	9.68	0.00	0.00	9.97	0.00	0.00	9.35	0.00	0.00
HR-SI	19.72	0.00	0.00	17.10	0.00	0.00	19.35	0.00	0.00	19.86	0.00	0.00	19.26	0.00	0.00
HR-VO	-0.67	0.50	0.58	-0.84	0.40	0.50	-0.44	0.66	0.71	-0.55	0.58	0.62	-0.50	0.62	0.66
HU-IN	7.12	0.00	0.00	6.65	0.00	0.00	7.00	0.00	0.00	7.65	0.00	0.00	6.60	0.00	0.00
HU-LR	6.31	0.00	0.00	6.66	0.00	0.00	5.90	0.00	0.00	6.81	0.00	0.00	6.37	0.00	0.00
HU-SI	11.40	0.00	0.00	10.27	0.00	0.00	10.83	0.00	0.00	11.90	0.00	0.00	11.49	0.00	0.00
HU-VO	-0.36	0.72	0.77	-0.23	0.82	0.82	-0.44	0.66	0.76	0.04	0.97	0.97	0.04	0.97	0.97
IN-LR	-1.83	0.07	0.08	-0.57	0.57	0.66	-2.26	0.02	0.03	-1.91	0.06	0.07	-0.91	0.36	0.45
IN-SI	5.60	0.00	0.00	4.63	0.00	0.00	4.91	0.00	0.00	5.46	0.00	0.00	6.70	0.00	0.00
IN-VO	-7.70	0.00	0.00	-7.06	0.00	0.00	-7.67	0.00	0.00	-7.74	0.00	0.00	-6.67	0.00	0.00
LR-SI	9.44	0.00	0.00	6.48	0.00	0.00	9.18	0.00	0.00	9.38	0.00	0.00	9.51	0.00	0.00
LR-VO	-6.92	0.00	0.00	-7.09	0.00	0.00	-6.60	0.00	0.00	-6.90	0.00	0.00	-6.45	0.00	0.00
SI-VO	-12.16	0.00	0.00	-10.83	0.00	0.00	-11.70	0.00	0.00	-12.12	0.00	0.00	-11.71	0.00	0.00

558



559 **Table S2c.** Table summarizing results of Dunn tests for pair-wise differences among clusters identified by affinity propagation for each of  
 560 the top five influential variables.

AFFINITY Pair	Center			Peak			Mean peak			Third quart			First quart		
	Z	P.unadj	P.adj	Z	P.unadj	P.adj	Z	P.unadj	P.adj	Z	P.unadj	P.adj	Z	P.unadj	P.adj
152-16	0.84	0.40	0.40	-0.43	0.66	0.66	0.24	0.81	0.81	2.33	0.02	0.02	0.20	0.84	0.84
152-616	16.64	0.00	0.00	14.23	0.00	0.00	15.60	0.00	0.00	18.09	0.00	0.00	15.68	0.00	0.00
16-616	22.88	0.00	0.00	21.43	0.00	0.00	22.33	0.00	0.00	22.56	0.00	0.00	22.51	0.00	0.00
152-812	7.95	0.00	0.00	7.59	0.00	0.00	7.57	0.00	0.00	8.88	0.00	0.00	7.73	0.00	0.00
16-812	9.94	0.00	0.00	11.37	0.00	0.00	10.31	0.00	0.00	8.97	0.00	0.00	10.60	0.00	0.00
616-812	-15.61	0.00	0.00	-11.83	0.00	0.00	-14.41	0.00	0.00	-16.52	0.00	0.00	-14.26	0.00	0.00

561

562 **ACKNOWLEDGEMENTS**

563 Land Acknowledgment: Cornell University is located on the traditional homelands of the  
564 Gayogohó:nq', members of the Haudenosaunee Confederacy, an alliance of six sovereign Nations  
565 with a historic and contemporary presence on this land. The Confederacy precedes the  
566 establishment of Cornell University, New York State, and the United States of America. We  
567 acknowledge the painful history of Gayogohó:nq' dispossession, and honor the ongoing connection  
568 of Gayogohó:nq' people, past and present, to these lands and waters. We likewise acknowledge the  
569 Dayak people who have tended and cared for the forests and waters of Kalimantan for millennia.  
570 We extend our deepest gratitude to the Tuanan community members who generously shared their  
571 deep knowledge of the forest and provided direct support in the field research, including Pak Nafisa,  
572 Pak Irwan, Pak Isman, Pak Rahmadt, Suga, Suwi, Pak Andre, and Awan. We thank the Tuanan  
573 Research Station's directors Sri Suci Utami Atmoko, Maria van Noordwijk, and Carel van Schaik for  
574 access to facilities and resources and for maintaining the long-term demographic records on the  
575 study animals and Erin Vogel for intellectual, logistical, and financial support that made the three-  
576 year study possible. We are grateful to all Tuanan researchers and particularly Lynda Dunkel and  
577 Brigitte Spillmann for their habituation efforts. Our Universitas Nasional counterparts Tomi  
578 Ariyanto, Jito Sugardjito, Sri Suci Utami Atmoko, Didik Prasetyo, and Astri Zulfa provided essential  
579 administrative and logistical support; and Indonesian partners including RISTEK-DIKTI, BKSDA,  
580 LIPI, KLHK, and the Borneo Orangutan Survival Foundation were vital in issuing permits and  
581 support. We are grateful to Beth Barrow, Alli Hofner, and Yann Quenet for collecting some of the  
582 recordings included in this study as well as Emily Martines and Jessica Lecorchick for their  
583 contributions to long call annotations. Lastly, we thank our Yang Center colleagues Holger Klinck  
584 and Russ Charif for valuable conversations at the early stages of acoustic analyses. This project  
585 would not have been possible without funding (PI and co-PIs indicated) from Rutgers University

586 (Erin Vogel), The Center for Human Evolutionary Studies (Erin Vogel), USAID (No. AID-497-A-  
587 13-00005: Erin Vogel, Robert Scott, Jito Sugardjito), and the American Association of University  
588 Women (WME).

589

590

591

## 592 REFERENCES

593 Alloghani, M., Al-Jumeily, D., Mustafina, J., Hussain, A., & Aljaaf, A. J. (2020). A Systematic Review  
594 on Supervised and Unsupervised Machine Learning Algorithms for Data Science. In  
595 *Unsupervised and Semi-Supervised Learning: Supervised and Unsupervised Learning for Data Science* (pp.  
596 3–21). Springer International Publishing.

597 Altmann, J. (1974). Observational study of behavior: Sampling methods. *Behaviour*, *49*, 227–267.

598 Araya-Salas, M., & Smith-Vidaurre, G. (2017). WarbleR: an r package to streamline analysis of  
599 animal acoustic signals. *Methods in Ecology and Evolution*, *8*(2), 184–191.

600 Arcadi, A. C. (1996). Phrase structure of wild chimpanzee pant hoots: Patterns of production and  
601 interpopulation variability. *American Journal of Primatology*, *39*(3), 159–178.

602 Askew, J. A., & Morrogh-Bernard, H. C. (2016). Acoustic characteristics of long calls produced by  
603 male orangutans (*Pongo pygmaeus wurmbii*): Advertising individual identity, context, and  
604 travel direction. *Folia Primatologica*, *87*(5), 305–319.

605 Blumstein, D. T., & Armitage, K. B. (1997). Does sociality drive the evolution of communicative  
606 complexity? A comparative test with ground-dwelling sciurid alarm calls. *The American*  
607 *Naturalist*, *150*(2), 179–200.

608 Bodenhofer, U., Kothmeier, A., & Hochreiter, S. (2011). APCluster: An R package for affinity  
609 propagation clustering. *Bioinformatics*, *27*, 2463–2464.

- 610 <https://doi.org/10.1093/bioinformatics/btr406>
- 611 Bradbury, J. W., & Vehrencamp, S. L. (2011). *Principles of animal communication (2nd ed.)*. Sinauer  
612 Associates.
- 613 Brady, B., Hedwig, D., Trygonis, V., & Gerstein, E. (2020). Classification of Florida manatee  
614 (*Trichechus manatus latirostris*) vocalizations. *The Journal of the Acoustical Society of America*, 147(3),  
615 1597–1606. <https://doi.org/10.1121/10.0000849>
- 616 Brock, G., Pihur, V., Datta, S., & Datta, S. (2008). clValid: An R package for Cluster Validation.  
617 *Journal of Statistical Software*, 25(4), 1–22.
- 618 Clink, D. J., Crofoot, M. C., & Marshall, A. J. (2018). Application of a semi-automated vocal  
619 fingerprinting approach to monitor Bornean gibbon females in an experimentally  
620 fragmented landscape in Sabah, Malaysia. *Bioacoustics*, 1–17.
- 621 Clink, D. J., & Klinck, H. (2020). Unsupervised acoustic classification of individual gibbon females  
622 and the implications for passive acoustic monitoring. *Methods in Ecology and Evolution*.
- 623 Cunningham, P., Cord, M., & Delany, S. (2008). Supervised learning. In M. Cord & P. Cunningham  
624 (Eds.), *Machine Learning Techniques for Multimedia*. Springer. [https://doi.org/10.1007/978-3-](https://doi.org/10.1007/978-3-540-75171-7_2)  
625 [540-75171-7\\_2](https://doi.org/10.1007/978-3-540-75171-7_2)
- 626 Cusano, D. A., Noad, M. J., & Dunlop, R. A. (2021). Fuzzy clustering as a tool to differentiate  
627 between discrete and graded call types. *JASA Express Letters*, 1(6), 061201.
- 628 Davila Ross, M., & Geissmann, T. (2007). Call diversity of wild male orangutans: A phylogenetic  
629 approach. *American Journal of Primatology*, 69(3), 305–324.
- 630 Elie, J., & Theunissen, F. (2016). The vocal repertoire of the domesticated zebra finch: A data-driven  
631 approach to decipher the information-bearing acoustic features of communication signals.  
632 *Animal Cognition*, 19(2), 285–315.
- 633 Erb, W. M., Barrow, E. J., Hofner, A. N., Utami-Atmoko, S. S., & Vogel, E. R. (2018). Wildfire

- 634 smoke impacts activity and energetics of wild Bornean orangutans. *Scientific Reports*, 8(1),  
635 7606. <https://doi.org/10.1038/s41598-018-25847-1>
- 636 Fedurek, P., Zuberbühler, K., & Dahl, C. D. (2016). Sequential information in a great ape utterance.  
637 *Scientific Reports*, 6, 38226.
- 638 Fischer, J., Wadewitz, P., & Hammerschmidt, K. (2017). Structural variability and communicative  
639 complexity in acoustic communication. *Animal Behaviour*.
- 640 Fournet, M. E., Szabo, A., & Mellinger, D. K. (2015). Repertoire and classification of non-song calls  
641 in Southeast Alaskan humpback whales (*Megaptera novaeangliae*). *The Journal of the Acoustical*  
642 *Society of America*, 137(1), 1–10. <https://doi.org/10.1121/1.4904504>
- 643 Freeberg, T. M., Dunbar, R. I. M., & Ord, T. J. (2012). Social complexity as a proximate and ultimate  
644 factor in communicative complexity. *Philosophical Transactions of the Royal Society London*  
645 *Biological Sciences*, 367(1597), 1785–1801.
- 646 Frey, B., & Dueck, D. (2007). Clustering by passing messages between data points. *Science*, 315(5814),  
647 972–976.
- 648 Fuller, J. L. (2014). The vocal repertoire of adult male blue monkeys (*Cercopithecus mitis*  
649 *stulmanni*): A quantitative analysis of acoustic structure. *American Journal of Primatology*, 76(3),  
650 203–216. <https://doi.org/10.1002/ajp.22223>
- 651 Gamer, M., Lemon, J., Fellows, I., & Singh, P. (2012). *irr: Various coefficients of interrater reliability and*  
652 *agreement*.
- 653 Garland, E., Castellote, M., & Berchok, C. (2015). Beluga whale (*Delphinapterus leucas*)  
654 vocalizations and call classification from the eastern Beaufort Sea population. *The Journal of*  
655 *the Acoustical Society of America*, 137(6), 3054–3067.
- 656 Greene, D., Cunningham, P., & Mayer, R. (2008). Unsupervised learning and clustering. In M. Cord  
657 & P. Cunningham (Eds.), *Machine Learning Techniques for Multimedia*. Springer.

- 658 [https://doi.org/10.1007/978-3-540-75171-7\\_3](https://doi.org/10.1007/978-3-540-75171-7_3)
- 659 Hallgren, K. A. (2012). Computing inter-rater reliability for observational data: An overview and  
660 tutorial. *Tutorials in Quantitative Methods for Psychology*, 8(1), 23.
- 661 Hammerschmidt, K., & Fischer, J. (1998). The vocal repertoire of Barbary macaques: A quantitative  
662 analysis of a graded signal system. *Ethology*, 104(3), 203–216.
- 663 Hammerschmidt, K., & Fischer, J. (2019). Baboon vocal repertoires and the evolution of primate  
664 vocal diversity. *Journal of Human Evolution*, 126, 1–13.  
665 <https://doi.org/10.1016/j.jhevol.2018.10.010>
- 666 Hedwig, D., Verahrami, A. K., & Wrege, P. H. (2019). Acoustic structure of forest elephant rumbles:  
667 A test of the ambiguity reduction hypothesis. *Animal Cognition*, 22(6), 1115–1128.  
668 <https://doi.org/10.1007/s10071-019-01304-y>
- 669 Huijser, L. A. E., Estrade, V., Webster, I., Mouysset, L., Cadinouche, A., & Dulau-Drouot, V.  
670 (2020). Vocal repertoires and insights into social structure of sperm whales (*Physeter*  
671 *macrocephalus*) in Mauritius, southwestern Indian Ocean. *Marine Mammal Science*, 36(2), 638–  
672 657. <https://doi.org/10.1111/mms.12673>
- 673 Janik, V. M. (1999). Pitfalls in the categorization of behaviour: A comparison of dolphin whistle  
674 classification methods. *Animal Behaviour*, 57(1), 133–143.
- 675 Jones, A. E., ten Cate, C., & Bijleveld, C. C. J. H. (2001). The interobserver reliability of scoring  
676 sonagrams by eye: A study on methods, illustrated on zebra finch songs. *Animal Behaviour*,  
677 62(4), 791–801.
- 678 K. Lisa Yang Center for Conservation Bioacoustics. (2019). *Raven Pro: Interactive Sound Analysis*  
679 *Software (Version 1.6.1) [Computer software]*. Ithaca, NY: The Cornell Lab of Ornithology. Available  
680 from <http://ravensoundsoftware.com>
- 681 Kassambara, A., & Mundt, F. (2020). *factoextra: Extract and Visualize the Results of Multivariate Data*

- 682           *Analyses*. <http://www.sthda.com/english/rpkgs/factoextra>
- 683   Kershenbaum, A., Blumstein, D., Roch, M., Akçay, Ç., Backus, G., Bee, M., Bohn, K., Cao, Y.,  
684           Carter, G., Cäsar, C., Coen, M., DeRuiter, S., Doyle, L., Edelman, S., Ferrer-i-Cancho, R.,  
685           Freeberg, T., Garland, E., Gustison, M., Harley, H., ... Zamora-Gutierrez, V. (2016).  
686           Acoustic sequences in non-human animals: A tutorial review and prospectus. *Biol Rev Camb*  
687           *Philos Soc*, 91(1), 13–52.
- 688   Landis, J. R., & Koch, G. G. (1977). The measurement of observer agreement for categorical data.  
689           *Biometrics*, 33(1), 159–174.
- 690   Lattenkamp, E. Z. (2019). The Vocal Repertoire of Pale Spear-Nosed Bats in a Social Roosting  
691           Context. *Frontiers in Ecology and Evolution*, 7, 14.
- 692   Light, R. J. (1971). Measures of response agreement for qualitative data: Some generalizations and  
693           alternatives. *Psychological Bulletin*, 76(5), 365.
- 694   MacKinnon, J. (1977). A comparative ecology of Asian apes. *Primates*.
- 695   Madhusudhana, S. K., Chakraborty, B., & Latha, G. (2019). Humpback whale singing activity off the  
696           Goan coast in the Eastern Arabian Sea. *Bioacoustics*, 28(4), 329–344.  
697           <https://doi.org/10.1080/09524622.2018.1458248>
- 698   Maechler, M., Rousseeuw, P., Struyf, A., Hubert, M., & Hornik, K. (2021). *cluster: Cluster Analysis*  
699           *Basics and Extensions*. <https://CRAN.R-project.org/package=cluster>
- 700   Marler, P., & Hobbett, L. (1975). Individuality in a long-range vocalization of wild chimpanzees.  
701           *Zeitschrift Für Tierpsychologie*, 38(1), 97–109.
- 702   Marler, P., Kavanaugh, J. F., & Cutting, J. E. (1975). On the origin of speech from animal sounds. In  
703           *On the origin of speech from animal sounds*. MIT Press.
- 704   Marshall, J., & Marshall, E. (1976). Gibbons and their territorial songs. *Science*, 193(4249), 235–237.
- 705   McComb, K., & Semple, S. (2005). Coevolution of vocal communication and sociality in primates.

- 706 *Biol Lett*, 1(4), 381–385.
- 707 McInnes, L., Healy, J., & Melville, J. (2018). UMAP: Uniform Manifold Approximation and  
708 Projection for Dimension Reduction. *ArXiv*, 1802.03426v3.
- 709 Meyer, D., Dimitriadou, E., Hornik, K., Weingessel, A., & Leisch, F. (2021). *e1071: Misc functions of*  
710 *the Department of Statistics, probability*. <https://CRAN.R-project.org/package=e1071>
- 711 Mitra Setia, T., & van Schaik, C. P. (2007). The response of adult orang-utans to flanged male long  
712 calls: Inferences about their function. *Folia Primatologica*, 78(4), 215–226.
- 713 Odom, K., Araya-Salas, M., Morano, J., Ligon, R., Leighton, G., Taff, C., Dalziell, A., Billings, A.,  
714 Germain, R., Pardo, M., de Andrade, L., Hedwig, D., Keen, S., Shiu, Y., Charif, R., Webster,  
715 M., & Rice, A. (2021). Comparative bioacoustics: A roadmap for quantifying and comparing  
716 animal sounds across diverse taxa. *Biol Rev Camb Philos Soc*.
- 717 Ogle, D. H., Doll, J. C., Wheeler, P., & Dinno, A. (2022). *FSA: Fisheries Stock Analysis*.  
718 <https://github.com/fishR-Core-Team/FSA>
- 719 Sadhukhan, S., Hennelly, L., & Habib, B. (2019). Characterising the harmonic vocal repertoire of the  
720 Indian wolf (*Canis lupus pallipes*). *PLOS ONE*, 14(10), e0216186.  
721 <https://doi.org/10.1371/journal.pone.0216186>
- 722 Sainburg, T., Thielk, M., & Gentner, T. (2020). Finding, visualizing, and quantifying latent structure  
723 across diverse animal vocal repertoires. *PLoS Comput Biol*, 16(10), e1008228.
- 724 Schwing, R., Parsons, S., & Nelson, X. J. (2012). Vocal repertoire of the New Zealand kea parrot  
725 *Nestor notabilis*. *Current Zoology*.
- 726 Soltis, J., Alligood, C., Blowers, T., & Savage, A. (2012). The vocal repertoire of the Key Largo  
727 woodrat (*Neotoma floridana smalli*). *J Acoust Soc Am*, 132(5), 3550–3558.
- 728 Spillmann, B., Dunkel, L. P., van Noordwijk, M. A., Amda, R. N. A., Lameira, A. R., Wich, S. A., &  
729 van Schaik, C. P. (2010). Acoustic properties of long calls given by flanged male orang-utans



- 730 (*Pongo pygmaeus wurmbii*) reflect both individual identity and context. *Ethology*, 116(5), 385–395.
- 731 <https://doi.org/10.1111/j.1439-0310.2010.01744.x>
- 732 Spillmann, B., Willems, E. P., van Noordwijk, M. A., Setia, T. M., & van Schaik, C. P. (2017).
- 733 Confrontational assessment in the roving male promiscuity mating system of the Bornean
- 734 orangutan. *Behavioral Ecology and Sociobiology*, 71(1), 20.
- 735 Taylor, D., Dezechache, G., & Davila-Ross, M. (2021). Filling in the gaps: Acoustic gradation
- 736 increases in the vocal ontogeny of chimpanzees (*Pan troglodytes*). *Am J Primatol*, 83(5),
- 737 e23249.
- 738 Thiebault, A., Charrier, I., Pistorius, P., & Aubin, T. (2019). At sea vocal repertoire of a foraging
- 739 seabird. *Journal of Avian Biology*, 50(5).
- 740 Turesson, H., Ribeiro, S., Pereira, D., Papa, J., & de Albuquerque, V. (2016). Machine learning
- 741 algorithms for automatic classification of marmoset vocalizations. *PLoS One*, 11(9),
- 742 e0163041.
- 743 Vester, H., Hallerberg, S., Timme, M., & Hammerschmidt, K. (2017). Vocal repertoire of long-
- 744 finned pilot whales (*Globicephala melas*) in northern Norway. *J Acoust Soc Am*, 141(6), 4289.
- 745 Wadewitz, P., Hammerschmidt, K., Battaglia, D., Witt, A., Wolf, F., & Fischer, J. (2015).
- 746 Characterizing Vocal Repertoires—Hard vs. Soft Classification Approaches. *PLOS ONE*,
- 747 10(4), e0125785. <https://doi.org/10.1371/journal.pone.0125785>
- 748 Zhou, K., Fu, C., & Yang, S. (2014). Fuzziness parameter selection in fuzzy c-means: The
- 749 perspective of cluster validation. *Science China Information Sciences*, 57(11), 1–8.